



TIME-DEPENDENT VACUUM ULTRAVIOLET EMISSION OF HELIUM

(Thesis)

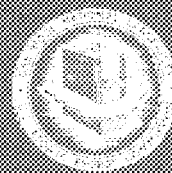
D. M. Bortell
G. S. Hurst
E. B. Wagner

OAK RIDGE NATIONAL LABORATORY
CENTRAL RESEARCH LIBRARY
DOCUMENT COLLECTION

LIBRARY LOAN COPY

DO NOT TRANSFER TO ANOTHER PERSON

If you wish someone else to see this
document, send in name with document
and the library will arrange a loan.



OAK RIDGE NATIONAL LABORATORY

OPERATED BY UNION-CARBIDE CORPORATION • FOR THE U.S. ATOMIC ENERGY COMMISSION

This report was prepared as an account of work sponsored by the United States Government. Neither the United States nor the United States Atomic Energy Commission, nor any of their employees, nor any of their contractors, subcontractors, or their employees, makes any warranty, express or implied, or assumes any legal liability or responsibility for the accuracy, completeness or usefulness of any information, apparatus, product or process disclosed, or represents that its use would not infringe privately owned rights.

ORNL-TM-3918

Contract No. W-7405-eng-26

HEALTH PHYSICS DIVISION

TIME-DEPENDENT VACUUM ULTRAVIOLET EMISSION OF HELIUM

D. M. Bartell, G. S. Hurst, and E. B. Wagner

Submitted by D. M. Bartell as a dissertation to the
Graduate School of The University of Kentucky
in partial fulfillment of the requirements
for the degree of
Doctor of Philosophy

SEPTEMBER 1972

OAK RIDGE NATIONAL LABORATORY
Oak Ridge, Tennessee 37830
operated by
UNION CARBIDE CORPORATION
for the
U. S. ATOMIC ENERGY COMMISSION

LOCKHEED MARTIN ENERGY RESEARCH LIBRARIES



3 4456 0514956 8

ACKNOWLEDGEMENTS

The authors earnestly thank J. T. Cox for design of the apparatus used in this work and J. P. Judish for operation and maintenance of the Van de Graaff accelerator. Recognition is due V. E. Anderson for his computer analysis of the data. The authors express gratitude to R. E. Knight, H. C. Schweinler, R. H. Ritchie, J. E. Talmage, N. Thonnard, T. E. Stewart, J. E. Parks, and H. L. Weidner for useful discussions concerning this work. H. C. Schweinler is due credit for calculating potential energy curves used in this work. The authors are thankful to A. E. Kingston and L. H. Toburen who supplied ionization cross sections. The authors appreciate the help of the Radiation Physics and High Voltage Laboratory staff members at Oak Ridge National Laboratory.

During this research work one of the authors (DMB) received financial support from a NASA Traineeship, a Dissertation Year Fellowship from the University of Kentucky, and an Oak Ridge Graduate Fellowship from Oak Ridge Associated Universities.

TABLE OF CONTENTS

	Page
LIST OF TABLES	vi
LIST OF ILLUSTRATIONS	vii
Section	
1. INTRODUCTION	1
2. EXPERIMENT	
2.1 Method	4
2.2 Results	14
3. THEORY	
3.1 The Steps of Radiation Action	37
3.2 Step-1 Primary Excitation and Ionization	37
3.3 Step-2 Electrons Slowing Down	40
3.4 Step-3 Radiative Decay	50
4. POTENTIAL SURFACES	53
5. DISCUSSION	
5.1 Proposed Model for the Vuv Emission	56
5.2 Proposed Model for the Jesse Effect	63
5.3 General Remarks	67
6. SUMMARY	68
APPENDIX	69
REFERENCES	96

LIST OF TABLES

Table	Page
1. Possible Sources of Observed Lines	18
2. Parameters for the Time Dependence of the 584-Å ^o Line	23
3. Parameters for the Time Dependence of the 601-Å ^o Peak	29
4. Parameters for the Time Dependence at 675 Å ^o and 825 Å	34
5. Parameters for the Time Dependence of Some Impurity Lines	36
6. Quantum Mechanical Differential Ionization Cross Sections for Protons in Helium	38
7. Classical Differential Ionization Cross Sections for Protons in Helium	39
8. Excitation Cross Sections for Protons in Helium	41
9. Average Number of Atoms Formed in Various Excited States Resulting from the Energy Degradation of a 1230-eV Electron	43
10. The Average Populations Resulting When One Proton Has a 1 cm Path in 10 ¹⁹ cm ⁻³ of Helium ...	47
11. Jesse Effect Rate for Argon in Helium	66

LIST OF ILLUSTRATIONS

Figure	Page
1. Apparatus Used in This Investigation	5
2. Gas Flow and Pumping System	6
3. Emission Cell	9
4. Schematic of Lifetime Experiment	11
5. Circuitry of CEM, Amplifier and Discriminator ...	12
6. Time Resolution of the Lifetime Apparatus	15
7. Emission Spectra of Proton-Excited Helium	17
8. Time Dependence of the 584-Å Line	20
9. Deconvolution of the Lifetime Data Shown in Figure 8	21
10. Pressure Dependence of the 584-Å Decay Rate, u_1 . The Dotted Curve is a Straight Line Thru the Low Pressure Data Points	25
11. Time Dependence of the 601-Å Peak	26
12. Pressure Dependence of the Decay Rate, u_2 , of the Main Component of the 601-Å Peak	28
13. Time Dependence at 675 Å and 825 Å	30
14. Pressure Dependence of the Fast Component at 675 Å	31
15. Wavelength Dependence of the Fast Component at 102 Torr	32
16. Pressure Dependence of the Decay Rate, u_4 , of the Main Component at 675 Å and 825 Å	35
17. Number of Excited Atoms per Incident Electron as a Function of Initial Electron Energy	44
18. The Energy Degradation When a 4-MeV Proton Loses a Fraction of Its Energy in Helium	46

Figure	Page
19. Relative Numbers of Various Excited States in Helium as a Function of Time	51
20. Potential-Energy Curves for Selected States of He ₂ : (a) Hypothetical curves; (b) refs. 47, 48, 49, and 50; (c) and (d) ref. 51; (e) ref. 54; (f) ref. 53; (g) ref. 52	54
21. Energy Pathways Model	57
22. Intensity Divided by Pressure Plotted as a Function of Pressure for the Helium 584-Å Resonance Line	59
23. Intensity Divided by Pressure Plotted as a Function of Pressure for the Vuv Emission Continuum of Helium	62

SECTION 1

INTRODUCTION

One fruitful method for studying the interaction of radiation with matter consists of examining the initial and the final states of the radiation-matter system. Another approach, of which this dissertation is an example, consists of observing many of the elementary processes occurring between the initial and the final states. These energy pathways studies in helium are especially meaningful because other theoretical and experimental investigations provide much additional input data.

Ionization occurs when radiation interacts with matter, and many experimentalists have measured the average energy expended by the radiation per ion pair it produces (W value). These W values are characteristic of the radiation-matter system under study; for 5-MeV alpha particles the W value of pure helium is 46 eV per ion pair.¹ Since the ionization potential of helium is only 25 eV, it is possible that nearly half the energy expended by the alpha particle is dissipated via pathways other than ionization.

About twenty years ago Jesse and Sadauskis² discovered a peculiar effect as they irradiated certain binary mixtures of gases with 5-MeV alpha particles. For instance, to helium, whose W value they measured to be 41.3 eV per ion pair, they

added a small amount of argon (0.13%). A large increase in ionization yield caused the W value to decrease to 29.7 eV per ion pair. There are differences of opinion^{2,3} concerning the explanation of these Jesse effects.

The light emitted in the vacuum ultraviolet (vuv) region by helium has been studied using gas discharge, spark, and microwave excitation.⁴⁻¹⁴ The light consists of atomic lines and broad molecular continua. There are conflicts of opinions concerning the atomic precursors and the processes involved in the creation of these continua.^{15,16}

The above two paragraphs cite but two examples of studies to obtain additional information on pathways not involving direct ionization. It suffices here to state that the models suggested for ionization and light emission phenomena are in conflict. In search of a unifying model for a given radiation-matter system, G.S. Hurst initiated a systematic study of elementary radiation (swift monoenergetic charged particles) reacting with elementary matter (mainly the noble gases). At the University of Kentucky in Lexington and at Oak Ridge National Laboratory investigations have been made and are continuing. The measurements accomplished are:

1. W values of the pure noble gases.¹⁷
2. The intensity of the vuv light as a function of wavelength for the same noble gases.¹⁸⁻²²
3. The fraction of energy lost by the charged particles that goes into vuv light emission

$(d\epsilon/dx)$.^{18,19,23,24}

4. The formation and decay times of the emission spectra at different wavelengths.²⁵
5. Jesse effects¹⁷ due to the addition of impurities.
6. The quenching of the light with the addition of the same impurities.²⁶

All these experiments are done over a wide range of pressures (under similar conditions) and under conditions where the charged particles lose only a small fraction of their energy in the gas. The experimental data obtained from the above measurements are coupled with a) theory and b) literature to suggest the radiation action model.

In the present work the time dependence of the vuv emission from proton-excited helium was measured, the initial steps of the action of protons in helium was treated theoretically and information on molecular helium's potential surfaces was assembled. These inputs were combined with W-value measurements and with other emission studies to suggest an energy-pathways model for the vuv continuum and the Jesse effect in helium.

SECTION 2

EXPERIMENT

2.1 Method

The apparatus used in this investigation is displayed in Figure 1. Bursts of protons from a Van de Graaff accelerator are detected with a time pickoff unit. Some of the protons scattered by a gold foil enter the W cell for ionization measurements. Rotating the gold foil out of the beam allows the protons to enter the emission cell. The vuv light emitted by the gas in the emission cell was analyzed with a monochromator and a single photon detector. Light intensity can be studied as a function of wavelength or as a function of time at a given wavelength. The simple geometry apparatus can be attached at the viewing port for absolute light intensity measurements. Emission stimulated by discharge excitation can be compared with the emission stimulated by proton excitation by attaching the discharge lamp at the viewing port. It is evident that all six of the measurements mentioned in the introduction can be made with this single system.

The complicated gas flow and pumping system of Figure 2 is unavoidable when observing vuv radiation, and when using a single photon detector and a Van de Graaff accelerator both of which require vacuum operation. The Roots blower is a Leybold-Hereaus type WS 700 backed with a DK-180 forepump.

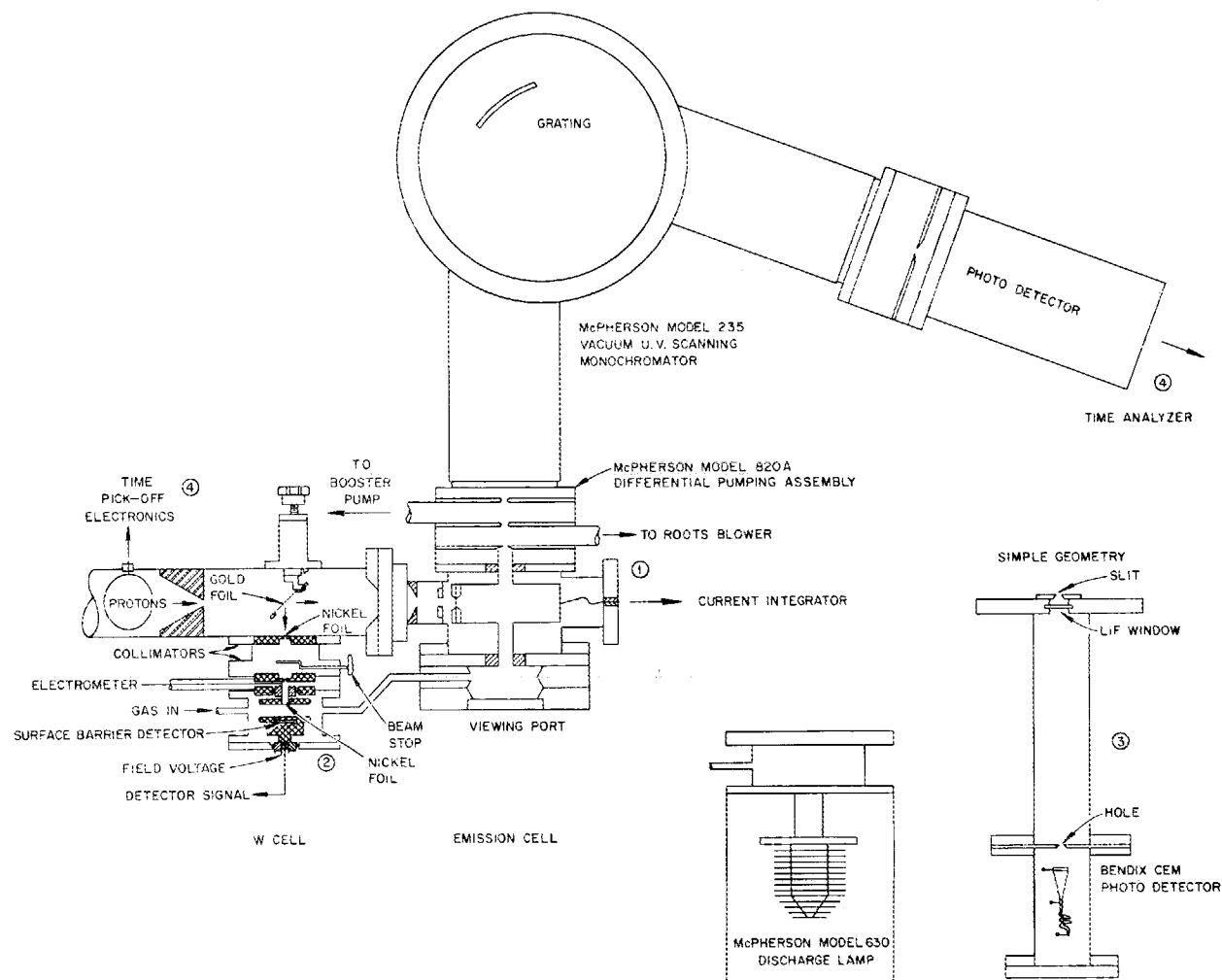


Figure 1. Apparatus Used in This Investigation.

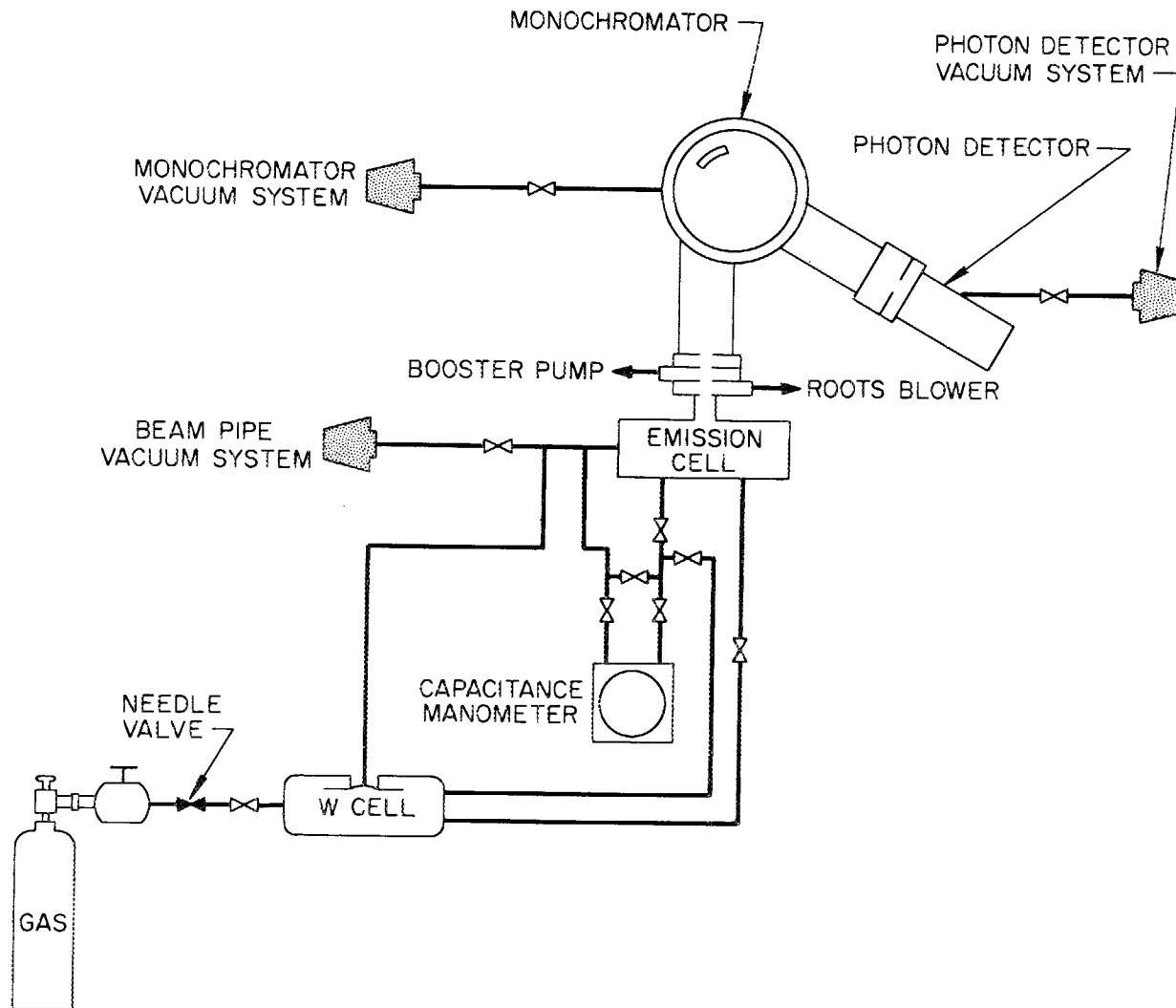


Figure 2. Gas Flow and Pumping System.

The monochromator pressure was at 5×10^{-4} Torr when the emission cell contained 300 Torr of helium with pumping done through a 50 micron by 1 cm monochromator entrance slit. For pressures above 300 Torr a 10 micron by 1 cm slit was used. By using short gas lines, stainless steel diaphragm valves, an ultra-high-purity pressure reducer, epoxy to seal porous insulators, and an MKS baratron for pressure determination, we maintained gas purity with no charcoal or molecular sieve traps. A good grade of helium (purity 99.9999%) was used. The flow rates used were dictated by the pressure in the emission cell and the size of the exit orifice (the monochromator entrance slit). With slit dimensions of 50 microns by 1 cm and 150 Torr of helium in the emission cell, the flow was 700 standard cc per minute as measured by a thermal conductivity flow meter.

The ORNL 3-MeV Van de Graaff accelerator was used as a source of 2-MeV protons. The beam was pulsed at the high-voltage terminal by electrostatically sweeping the beam across an aperture. The repetition rate was varied from 125 kHz to 7.81 kHz. Proton bursts were less than 50 nanoseconds in duration. The time averaged beam current was proportional to the pulse repetition rate, and at 125 kHz 0.4 microamperes was typical.

W-value experiments are a convenient way to verify the purity of the gas. For example, Parks¹⁷ observed that a 2% drop in W value is caused by the addition of only 5 ppm of

argon. Similar effects occur when other atomic or molecular gases are added to helium.^{1,2,17,18} Neon is the only known contaminant that does not cause a Jesse effect in helium.¹⁷

The W cell, Figures 1 and 2, is a parallel plate ionization chamber with a solid-state detector incorporated into the field-voltage plate. A small fraction of the incident protons were scattered into the W cell by a thin gold foil placed with its normal at 45° to the incident beam. Some of the Rutherford-scattered protons were collimated, entered the W cell through a nickel foil, lost a fraction of their energy in the gas, and struck the particle detector. Protons were counted by counting the signals from the detector. The energy expended per proton in the gas was reckoned using pressure and length measurements, tabulated stopping powers, and a normalization to nitrogen's W value. The total ion pairs produced were determined by using a vibrating reed electrometer. From these quantities the W value was calculated, as described by Parks.¹⁷

The emission cell, shown in Figure 3, was made from a block of stainless steel by boring out a cylinder for the proton-beam path. Protons entered the gas-filled cell through a 0.0001-inch havar foil. The foil was sealed with a lead gasket; other seals were made with viton "O" rings. The light emitted by the proton-excited helium entered the monochromator through the entrance slit. Visible light could be observed by looking into the viewing port. Qualitative

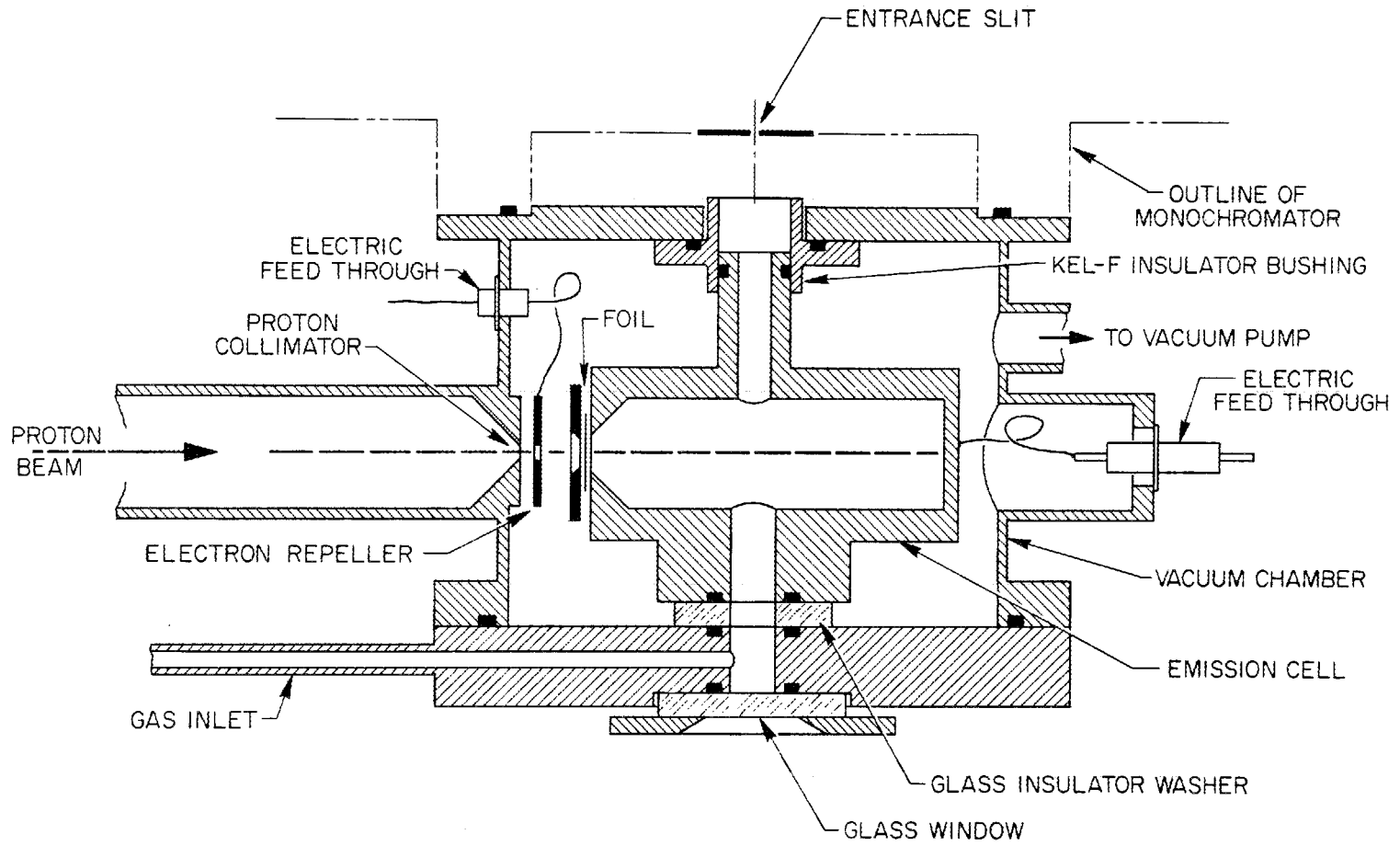


Figure 3. Emission Cell.

changes using different samples of helium were seen with the eye. At 1000 Torr pure helium appeared white; helium with traces of neon, peach; helium with traces of air, purple. These observations were crude compared with the sensitivity of the W-value measurement, but helped locate real and virtual leaks in the system before the W cell was operative. Emission spectra were obtained by recording the proton count rate as the grating rotated, Figure 4. The scanning monochromator was a McPherson model 235, differentially pumped at the entrance slit. The diffraction grating had 600 lines per mm, was blazed at $1500 \overset{\circ}{\text{Å}}$, and was in a Seya-Namioka geometrical arrangement. A Bendix channel electron multiplier (CEM) was used as a photon counter. A schematic of the CEM and the amplifier²⁷ is displayed in Figure 5.

The total electrical charge brought in by the incident proton beam was collected in the emission cell (isolated from ground) and conducted to an ammeter and current digitizer. We investigated whether charged particles were leaving the emission cell via escape routes such as electrons leaving the cell at the havar foil, or ions and electrons being swept out of the cell with the flowing gas. An electron repeller at a negative 45 volts relative to ground was sufficient to prevent electron escape. There was no evidence of ion flow.

In the lifetime experiment a burst of protons entered the emission cell at some instant in time, radiation action occurred, and at some later instant a photon was emitted.

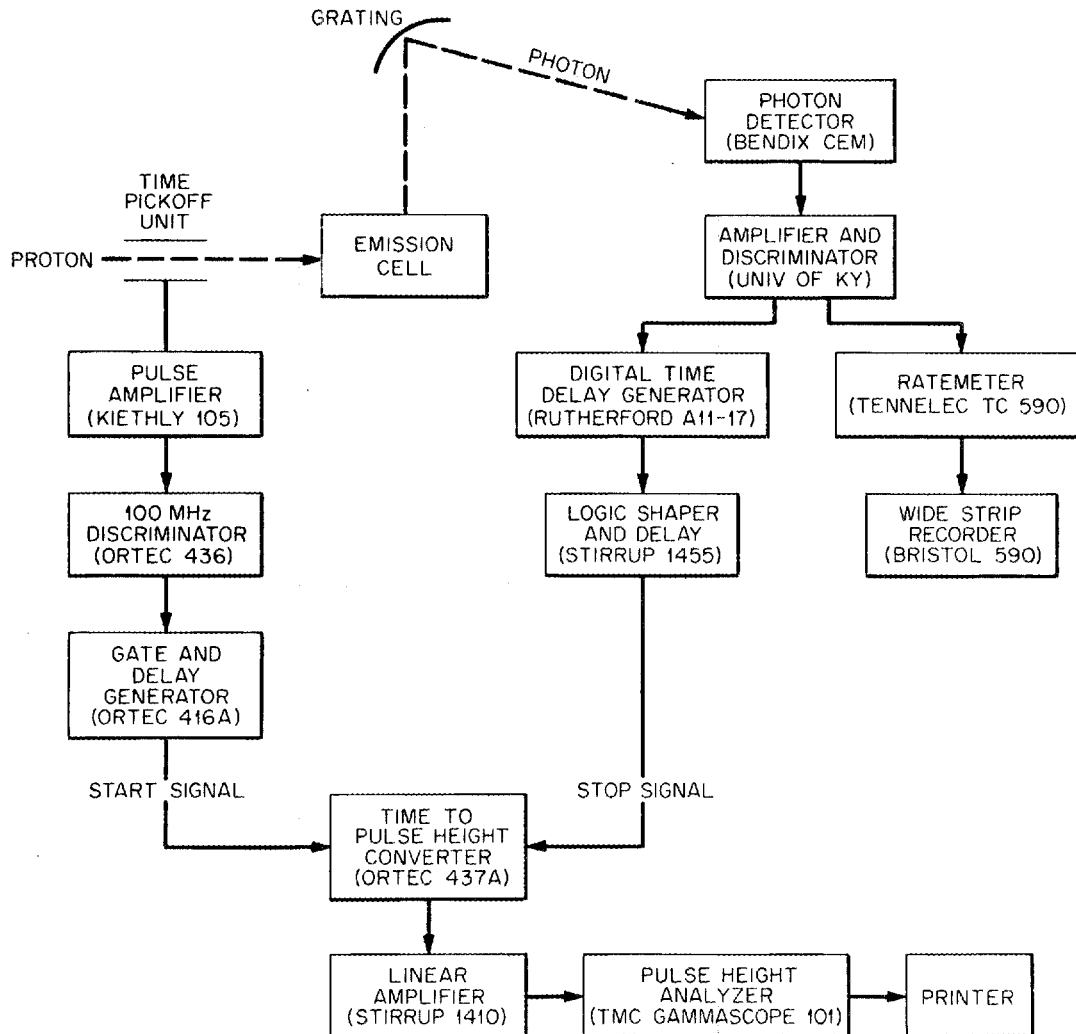


Figure 4. Schematic of Lifetime Experiment.

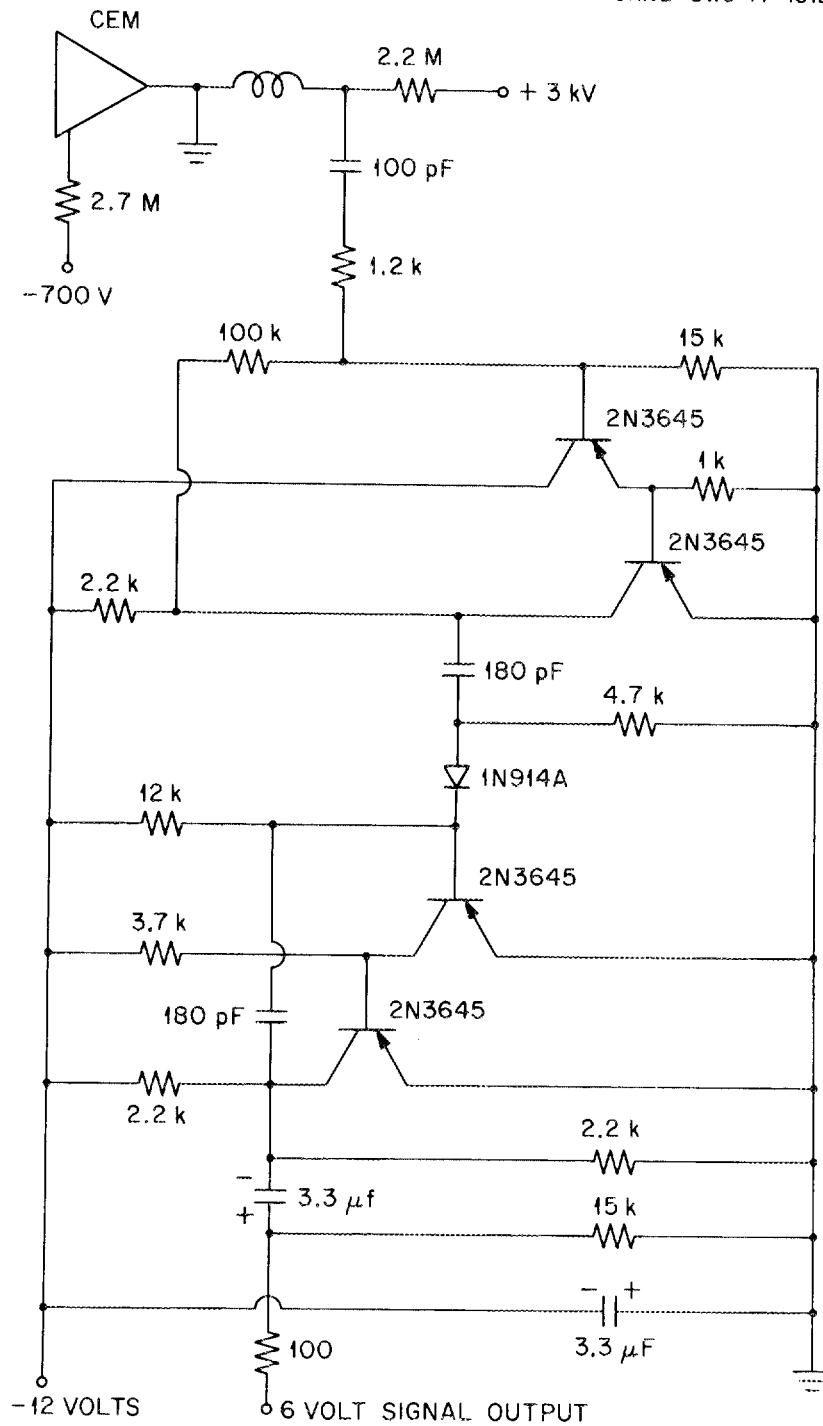


Figure 5. Circuitry of CEM, Amplifier and Discriminator.

The length of time between these two instants was measured repeatedly for a fixed pressure and wavelength. The resulting distribution of time periods revealed characteristics of the radiation action. The apparatus shown in Figure 4 allowed us to obtain conveniently these distributions of time periods. The time-pickoff unit for the start signal was an existing piece of hardware. It was a cylinder with a 1-inch inside diameter and a 12-inch length that was inside of and insulated from the beam pipe. When the burst of protons passed through this cylinder, the start pulse for this experiment was generated. The stop pulse was generated when a photon struck the CEM. Start and stop pulses were shaped before entering the time to pulse height converter (TPHC). The output pulse from the TPHC had a height proportional to the length of time between the two input pulses. Full scale range on the TPHC was variable from 50 nanoseconds to 80 microseconds. These time spans were adequate except for a couple of measurements at low pressures where the 80-microsecond span was not long enough. The pulse height analyzer had 100 channels of memory and stored one count in a particular channel when a pulse with a height corresponding to that channel was encountered. After accumulating enough data so that the peak of the distribution had at least 2,000 counts, we caused the printer to list the contents of the memory.

This time measuring system was calibrated by using two pulses from a single source and delaying one of the

pulses a desired length of time with a digital time delay generator. During this work the maximum variation in the calibration number was 3.6%. The system was linear to 0.2 microseconds on the TPHC 80-microsecond scale. The amount of this departure from linearity on all ranges was roughly proportional to the TPHC setting.

To determine the entire system's time resolution, we observed two relatively fast decay processes, nitrogen's emission lines at 1134 \AA and 1200 \AA . The natural lifetimes of the upper atomic states associated with these lines are less than 5 nanoseconds. We observed almost identical data at both wavelengths. Figure 6 illustrates measured and ideal response of the system at 1134 \AA . The smearing out of the time spectrum is about 100 nanoseconds. There may be complicated decay processes involved in the nitrogen emission making the prediction for an ideal experiment incorrect; however, the measurement did show that the time resolution was good to at least 100 nanoseconds.

If in the course of this lifetime investigation 2 photons from one burst of protons were incident on the CEM, we would have seen only the first photon, and this would have skewed the distribution in time. However, the CEM detected less than 1 photon per 10 proton bursts, assuring valid data, as can be argued from Poisson statistics.

2.2 Results

Since the objective of this work is the elucidation of

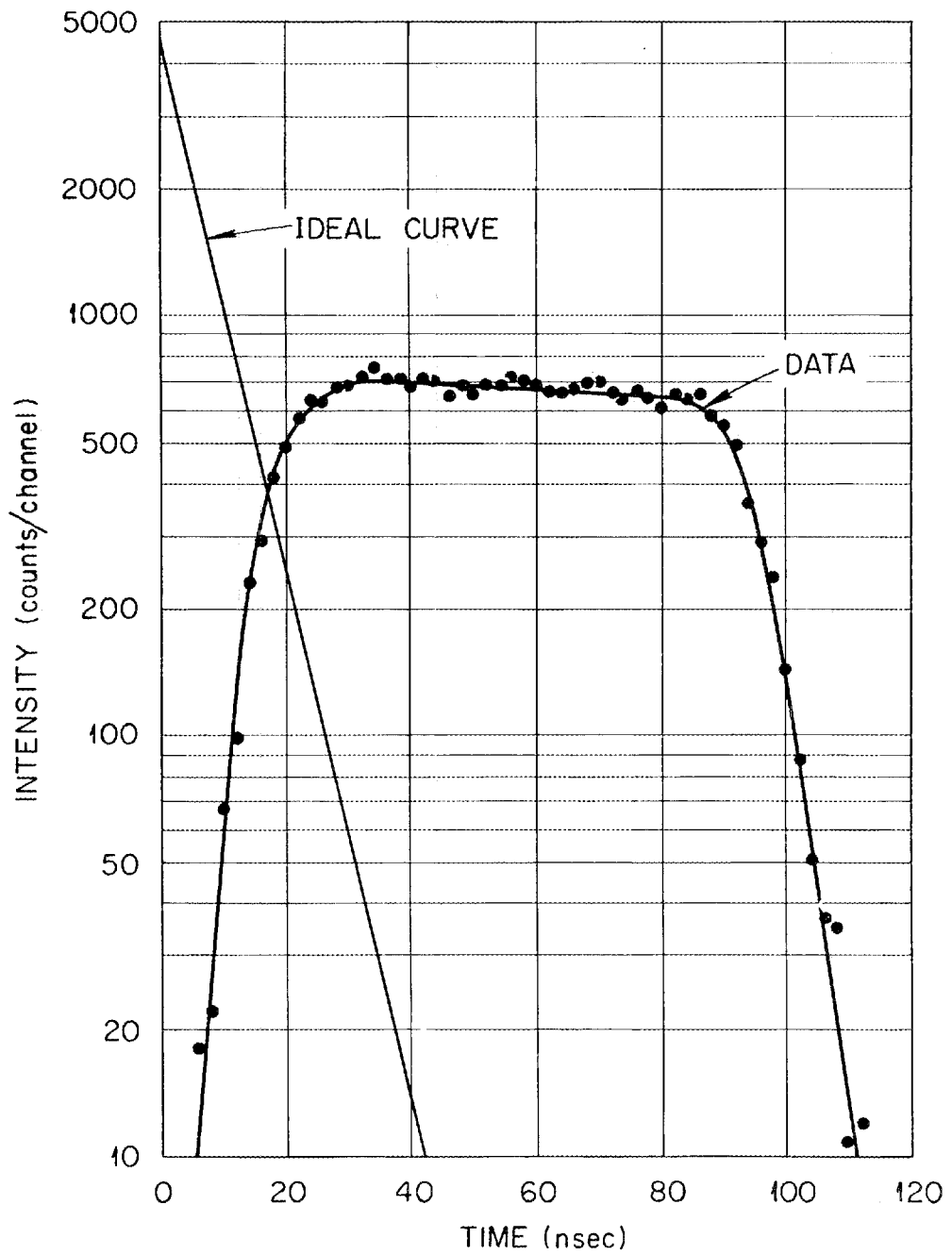


Figure 6. Time Resolution of the Lifetime Apparatus.

energy pathways following the interaction of charged particles with matter, we made many studies of the interaction of protons with helium gas. We measured the time dependence of monochromatic vuv emission at many wavelengths from proton excited helium gas at pressures from 5 to 1000 Torr (see appendix). For energy pathways studies, gas discharge excitation is inadequate. Gas discharge excitation depends on excitation mode (see Stewart's¹⁸ comparison of proton and discharge induced vuv emission for the noble gases), and it is limited to low pressures. With gas discharges the uncertain initial conditions (original energy of the electrons) complicate the theoretical analyses. However, emission studies done with monoenergetic proton excitation are reproducible and they can be done over a wide pressure range.

Furthermore, these emission processes involving excited atomic states can be correlated with ionization studies which involve the ionization continuum. The well-defined initial conditions of monoenergetic proton excitation invite theoretical treatment and permit simple estimations such as the optical approximation.²⁸

The 100 Torr spectrum (Figure 7) shows the 584-Å resonance line, the 601-Å peak with its small adjoining continuum, the 675-Å continuum extending from about 650 to 750 Å, the 800-Å continuum extending from 750 to 1000 Å and other atomic lines (Table 1). The atomic lines are more prominent at lower pressures, but the continua dominate at

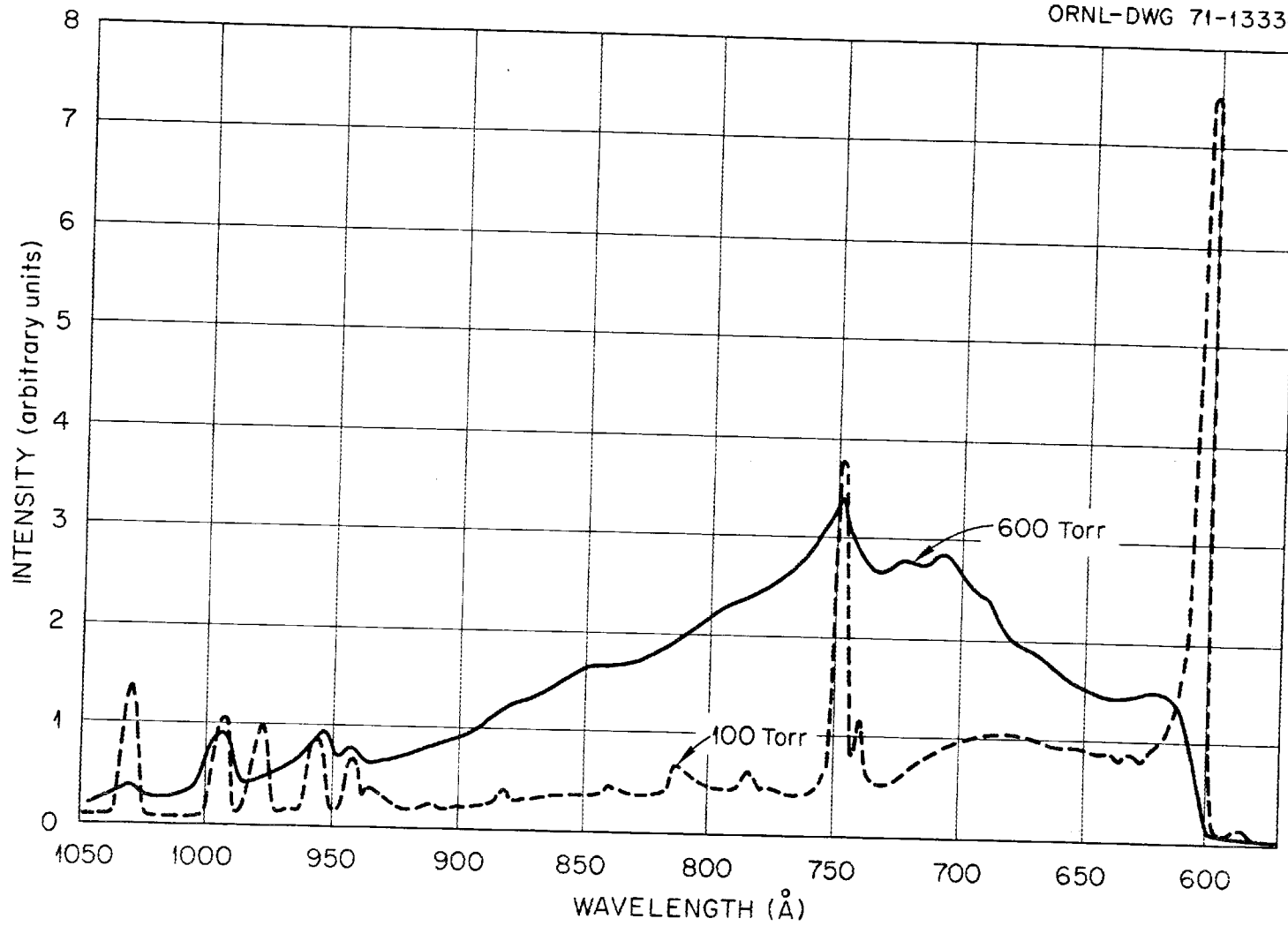


Figure 7. Emission Spectra of Proton-Excited Helium.

TABLE 1

POSSIBLE SOURCES OF OBSERVED LINES

Wavelength (Å)	Source
584	He I
601	He I
619	Ne I
736	Ne I
744	Ne I
770	O I
810	O I
835	N II or O II
858	N I or N II
869	N I
907	N I
929	H or O I
937	H, He II, or O I
951	He II, N I, O I, or H
971	H, He II, or O I
987	He II or O I
1025	He II, O I, or H
1038	N I or O I

higher pressures. These are nearly identical with the spectra obtained by Stewart.^{18,19,22}

Total-ionization (W value) measurements were made almost simultaneously with the lifetime data discussed below. These W values were in the range of 41.9 to 43.8 eV per ion pair, except at 50 Torr where the W value was 40.9 eV per ion pair (see Appendix). Variation of lifetime data with W-value are indicated later in this section.

The time resolved spectra of the $584\text{-}\overset{\circ}{\text{A}}$ resonance line was studied at pressures from 5 to 150 Torr. The line is the result of an allowed atomic transition to the ground state (2^1P to 1^1S). After excitation the intensity of emitted light increased rapidly to a maximum, within the time resolution of the system (0.15 μsec) and then decreased exponentially in time, as shown in Figure 8. The slope of a semilog plot of the intensity versus time is the decay rate.

We investigated whether the slope of these decay curves would be affected by our finite time resolution. The 135 Torr measurement, one of the fastest decays observed, was the trial case. A deconvolution procedure was carried out by using the spectrum shown in Figure 6, as a smearing function. For interpretational purposes, smooth curves were drawn through the input data. The resulting deconvolution is displayed as the points in Figure 9. Our decay-rate measurements are not noticeably affected by the finite time resolution.

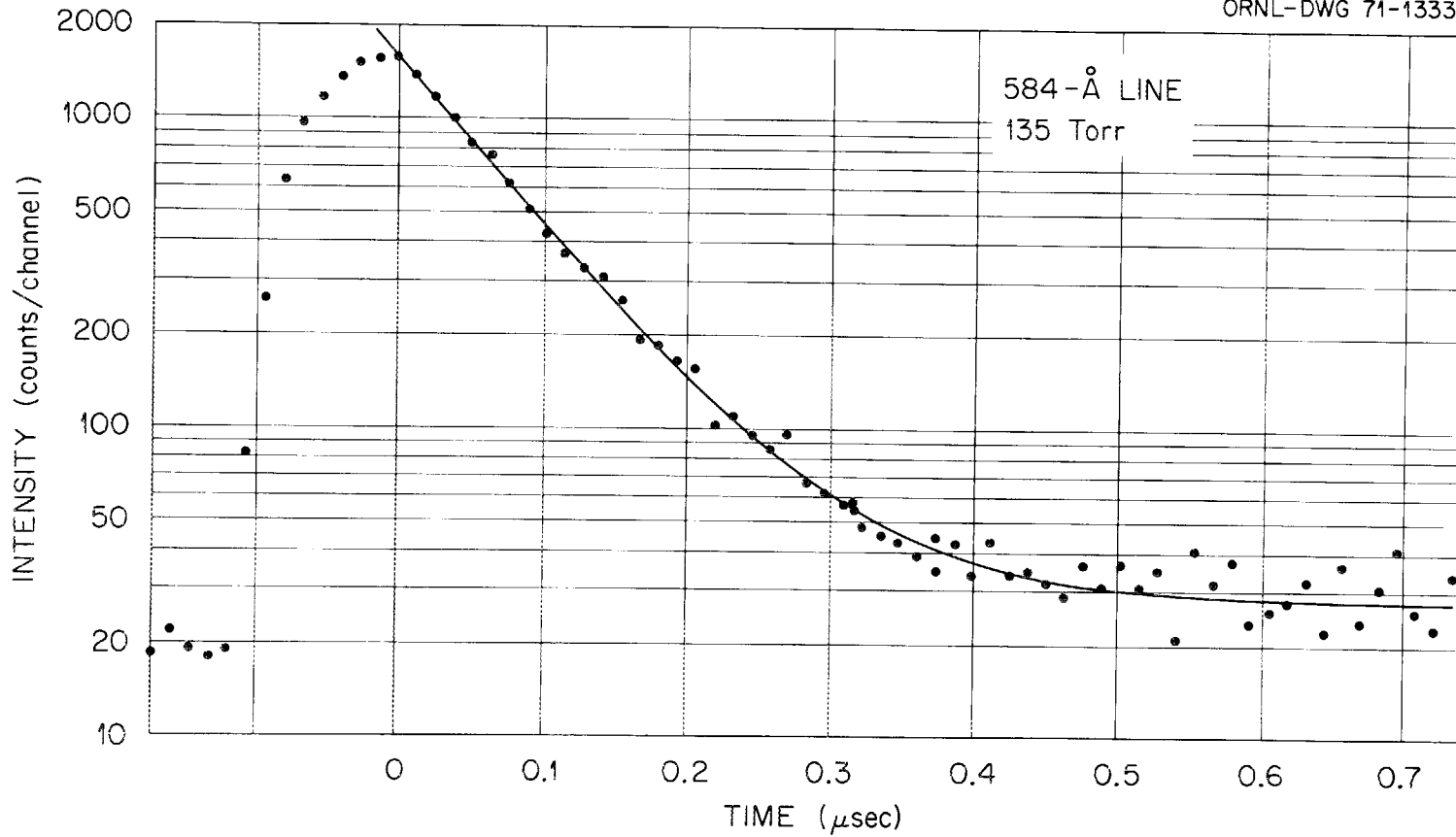


Figure 8. Time Dependence of the 584-Å Line.

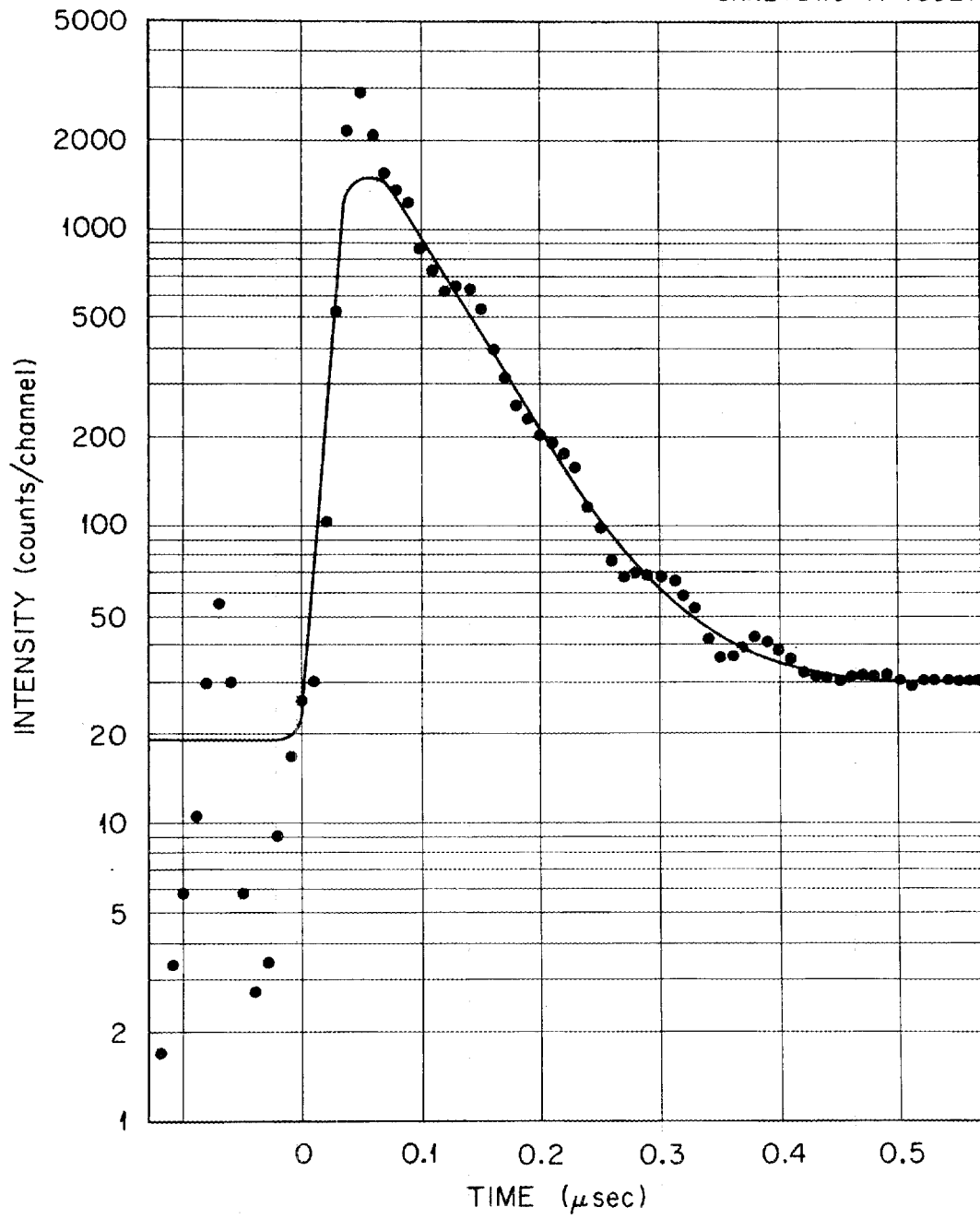


Figure 9. Deconvolution of the Lifetime Data Shown in Figure 8.

The slopes determined manually agreed with the computer least-squares fit to

$$I(t) = A_1 \exp(-u_1 t) + A_0.$$

$I(t)$ is the observed intensity of emitted light at time t . A_1 , A_0 , and u_1 are constants. The decay rate, u_1 , increases with pressure (Table 2).

The pressure dependence of the decay rate reveals information concerning the de-excitation mechanisms as shown below. The change in the number of atoms in the 2^1P excited state per cm^3 , dN^* , is

$$dN^* = - [\gamma + \beta(N) + BN + CN^2] N^* dt$$

where N is the density of ground state atoms. For this preliminary analysis radiation cascade into the 2^1P state was neglected. The constant γ is the rate for spontaneous de-excitation to the 2^1S state. B and C are rate coefficients. β is the effective rate for spontaneous de-excitation to the 1^1S ground state. An effective rate rather than the natural rate is used because the resulting $584\text{-}\overset{\circ}{\text{A}}$ photons are absorbed and re-emitted by neighboring ground state atoms many times (resonance trapped) before they escape from the gas cell thus making the rate slower. It is known from theory²⁹ that for a spectral line with only doppler and natural broadening (low gas densities) β varies as $1/N$ and that for a spectral line dominated by pressure broadening (high gas densities)

TABLE 2

CALCULATED PARAMETERS FOR TIME DEPENDENCE OF THE 584-Å LINE

Run No.	Pressure (Torr)	u_1 (10^6 sec^{-1})	A_1	A_0
157	5.4	3.02	973	-14
56	10	3.49	2690	4
47	24.5	4.29	3095	11
45	50	5.87	1699	6
153	71.2	7.28	1894	10
158	86.3	9.00	2618	21
154	102	9.73	2198	23
155	121	11.4	1772	26
156	135	12.8	1589	28
55B	151	13.8	1539	58

β is independent of pressure. However, the dependence of β on N is not known for the intermediate pressures of interest here. Following excitation, the time dependence of the observed 584-Å intensity, $I(t)$, is

$$I(t) = \frac{\beta D \exp - [\gamma + \beta(N) + BN + CN^2]}{\gamma + \beta(N) + BN + CN^2} + A_0$$

where D is the photon detection efficiency and A_0 is background. Therefore

$$u_1 = \gamma + \beta(N) + BN + CN^2$$

or

$$u_1 = \gamma + \beta(P) + \frac{BLP}{760} + \frac{CLP^2}{760^2}$$

where L is Loschmidt's number and P is the pressure in Torr. To determine the relative importance of the various de-excitation processes, the rate (Table 2) was plotted versus pressure, Figure 10. Both linear and quadratic terms are evident.

Time resolved spectra of the 601-Å peak were obtained in the pressure range of 50 to 1000 Torr, Figure 11. The rise times of these spectra were instantaneous within our time resolution. The decay was exponential but slow. In fact, the 50 and 100 Torr decay rates were too slow to be determined accurately with this system, as mentioned previously. Because there was a small secondary component in the decay, the data were fit to

ORNL-DWG 71-13328

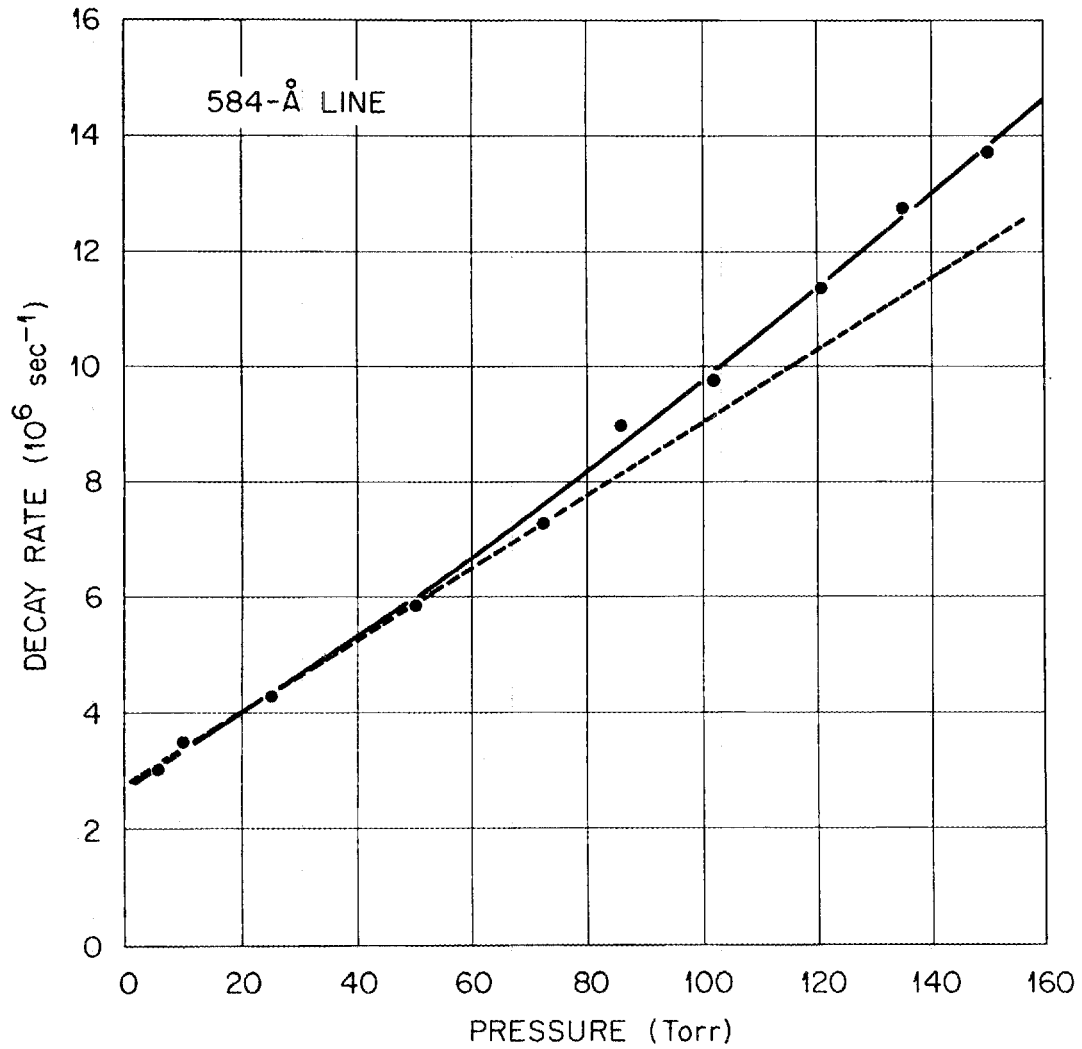


Figure 10. Pressure Dependence of the 584-Å Decay Rate, u_1 . The dotted curve is a straight line thru the low pressure data points.

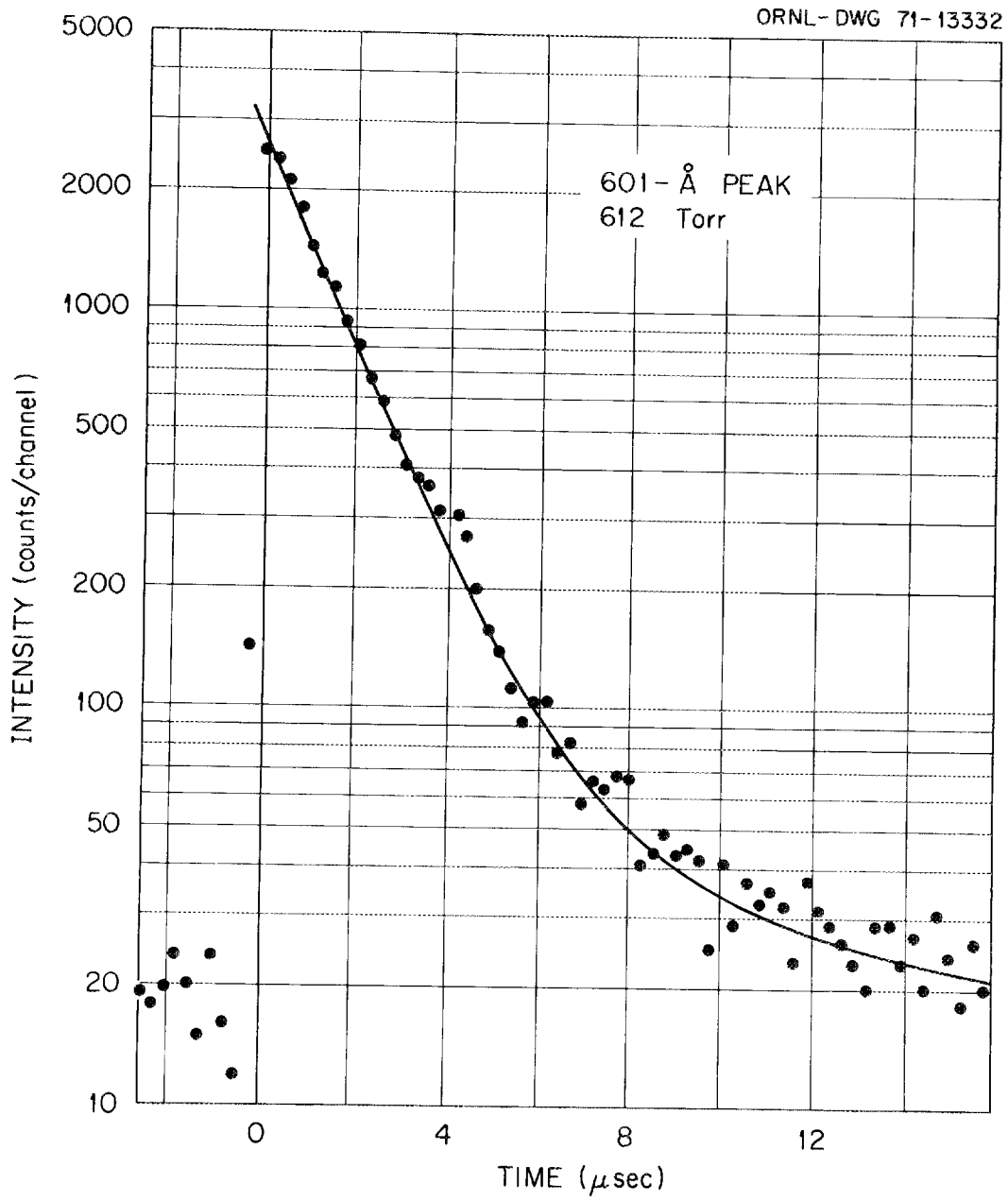


Figure 11. Time Dependence of the 601-Å Peak.

$$I(t) = A_2 \exp(-u_2 t) + A_3 \exp(-u_3 t).$$

Where u_2 is the decay rate of the main component. The u_3 , A_2 , and A_3 are other constants. Between 200 and 800 Torr the decay rate of the main component was proportional to the pressure squared (Figure 12, Table 3). The more impurities occurring in the gas sample, the lower the W value and emission intensity.¹⁸ Table 3 shows the changes in the time resolved spectra due to impurities. The decay rates at wavelengths corresponding to the half maxima of the 601-Å peak and the small adjoining continuum were slightly different than at the peak itself.

The time resolved spectra of the 675 and 800-Å continua are so similar that they will be discussed together. Both intensities built up to a maximum within the resolution time, decayed to half intensity rapidly (0.3 μ sec), and then completed the decay slowly (Figure 13). The fast decay component showed a definite pressure dependence between 100 and 600 Torr, but it was too fast for us to measure accurately (Figure 14). The total intensity of the fast component relative to the slow component is about 1:6 and constant with wavelength except in the region of 660 to 620 Å (Figure 15). The slow component was analyzed by omitting the very early part of the decay curve and fitting to

$$I(t) = A_4 \exp(-u_4 t) + A_5 \exp(-u_5 t).$$

The decay rate of the main component, u_4 , shows a pressure

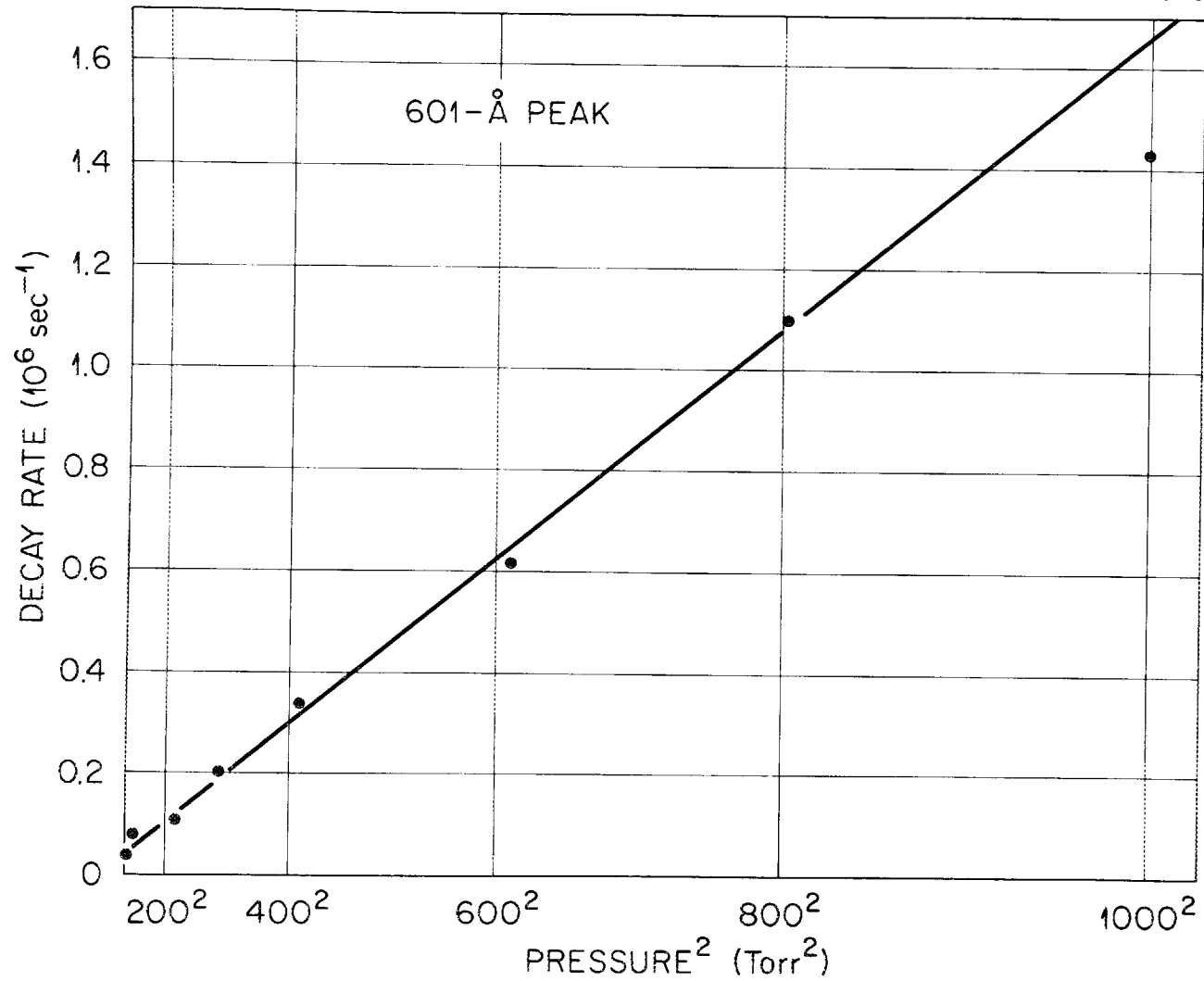


Figure 12. Pressure dependence of the Decay Rate, λ_2 , of the main component of the 601-Å Peak.

TABLE 3

PARAMETERS FOR THE TIME DEPENDENCE OF THE 601-Å PEAK

Run No.	Pressure (Torr)	u_2 (10^6 sec^{-1})	u_3 (10^6 sec^{-1})	A_2	A_3
55A	51	0.039	0.011	815	939
140	102	0.080	0.033	1697	3650
34 ^a	212	0.110	0.020	14619	300
175 ^b	202	0.120	0.036	8586	145
123 ^c	206	0.113	0.025	12934	277
124 ^d	207	0.108	0.002	7802	37
125 ^e	208	0.114	0.026	6794	154
126 ^f	208	0.120	0.039	1819	158
186	301	0.204	0.078	10751	409
31	416	0.341	0.032	2097	66
37	612	0.616	0.055	2681	51
179	803	1.10	0	1311	22
74	1002	1.43	0.115	2060	48

^a $w = 43.8$ eV per ion pair.

^b $w = 40.0$ eV per ion pair.

^c $w = 42.7$ eV per ion pair.

^d $_{596 \text{ Å}}, w = 42.7$ eV per ion pair.

^e $_{605 \text{ Å}}, w = 42.7$ eV per ion pair.

^f $_{620 \text{ Å}}, w = 42.7$ eV per ion pair.

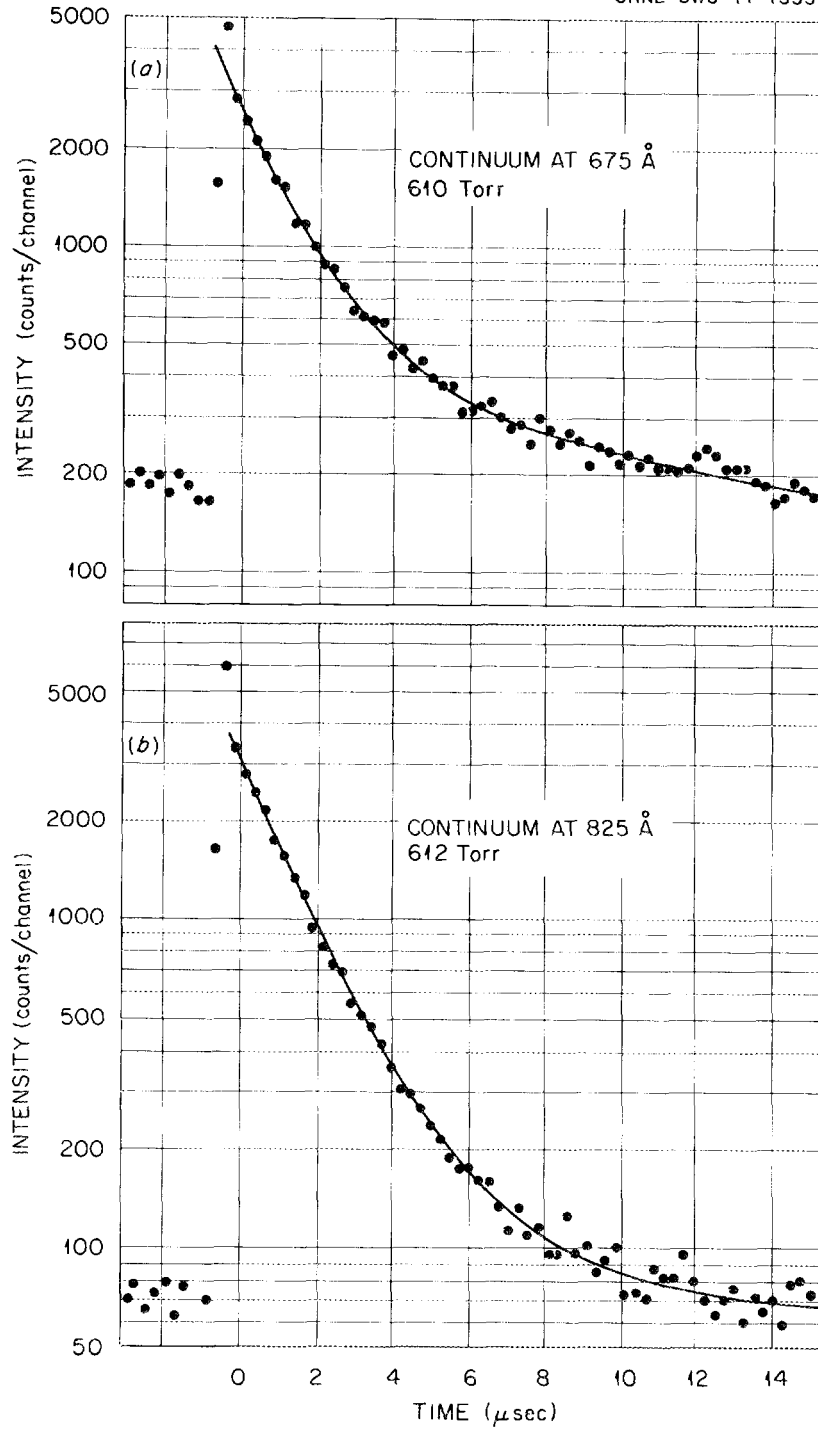


Figure 13. Time Dependence at 675 Å and 825 Å.

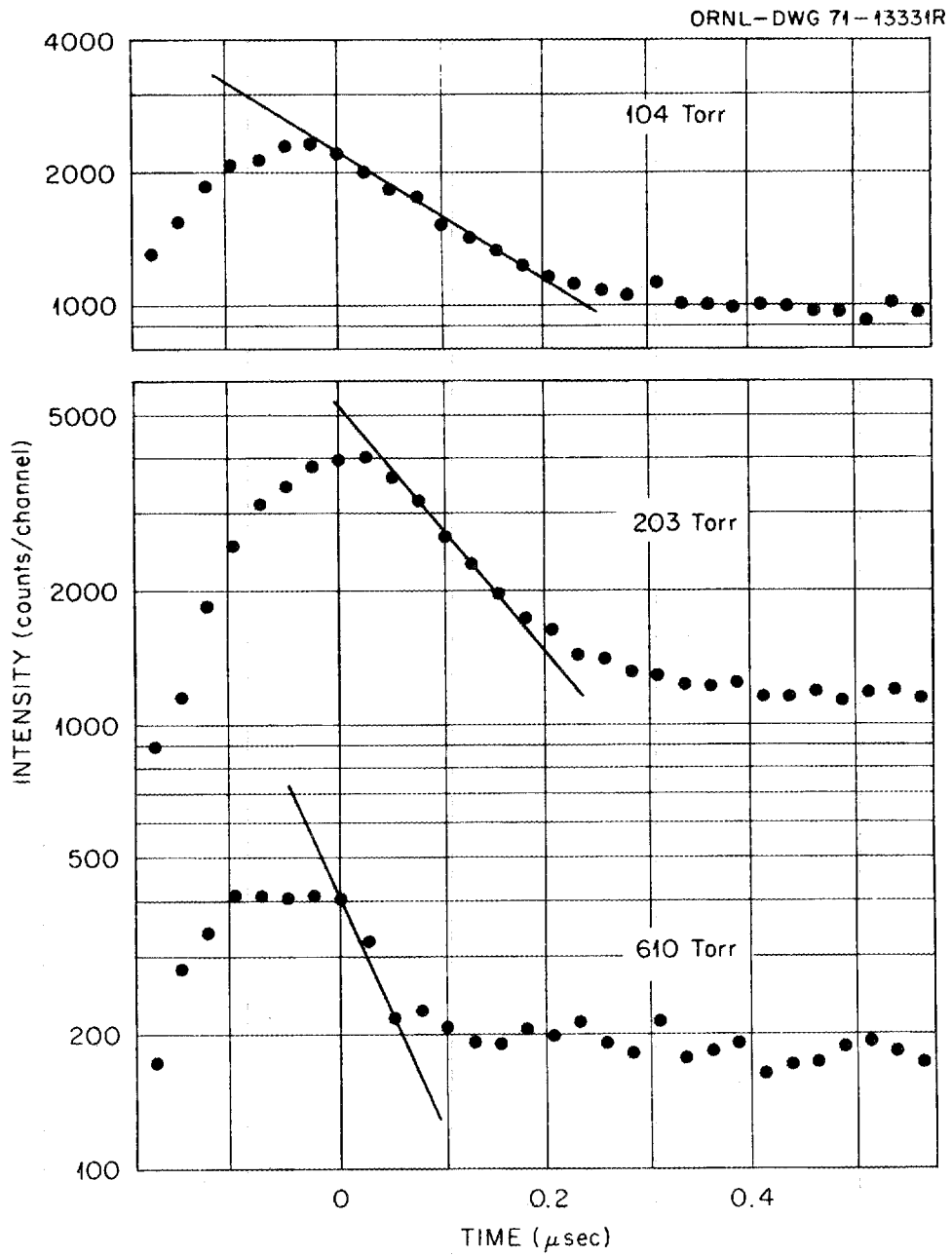


Figure 14. Pressure Dependence of the Fast Component at 675 \AA .

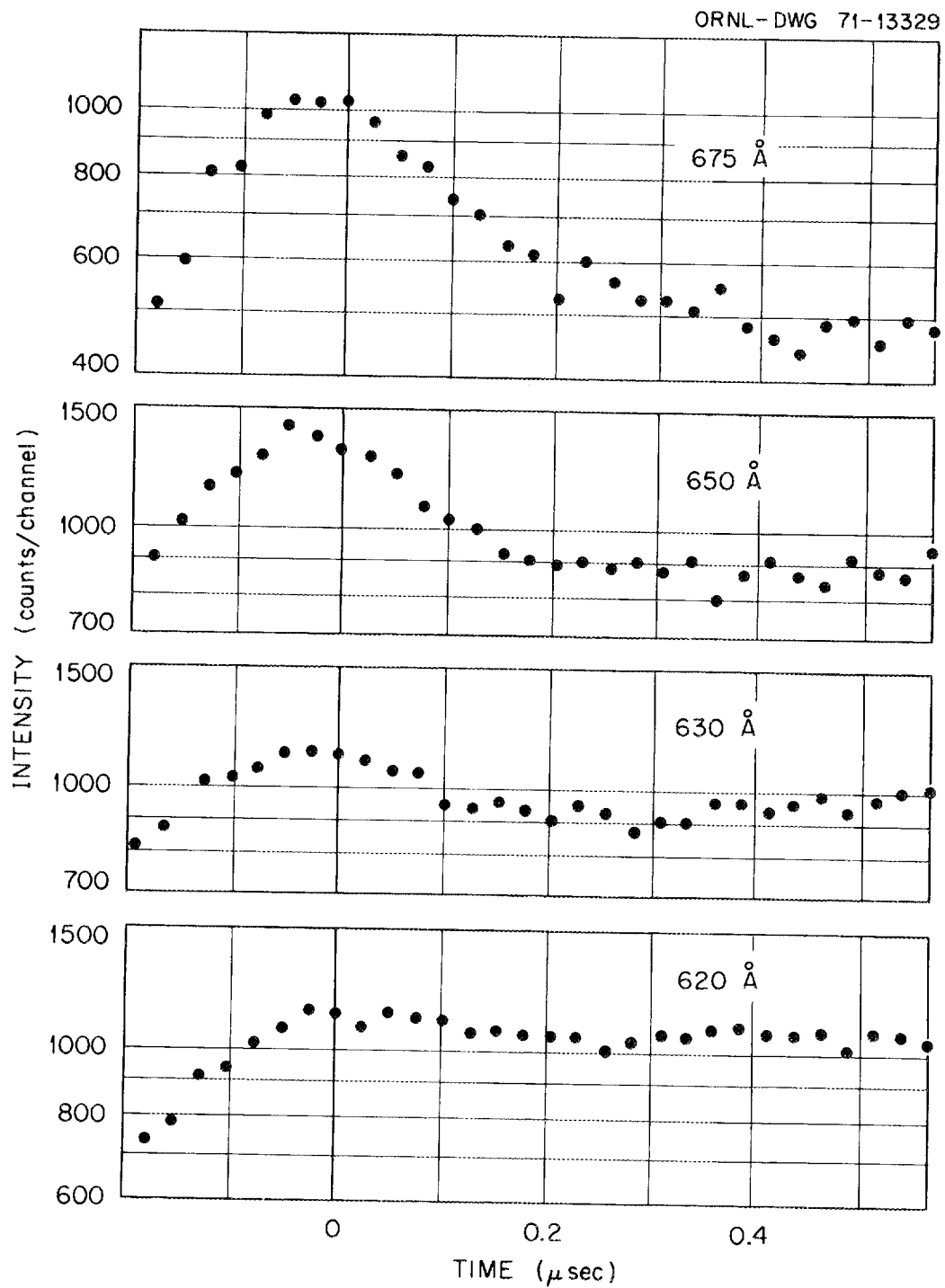


Figure 15. Wavelength Dependence of the Fast Component at 102 Torr.

dependence (Table 4 and Figure 16). Changes in the decay rate with gas purity can also be seen in Table 4.

We observed the time resolved spectra for five of the impurity lines (736, 744, 971, 987, and 1025 Å). These lines have a fast decay component and slower components similar to those of the 675 and 800-Å continua. The resulting decay rates shown in Table 5 were obtained by implementing the same analysis technique used on the 675 and 825-Å data. The W value of the gas used in making these measurements was 42.7 eV per ion pair.

The main decay rates reported (u_1 , u_2 , and u_4) were reproduceable to better than eight per cent with an absolute error of no more than ten per cent. Rates u_2 and u_4 at 50 Torr and 100 Torr are exceptions and are accurate to thirty per cent. This is because the primary component was so long-lived at these low pressures that the 80 μ sec time period was not long enough to separate accurately the primary component from the secondary component.

TABLE 4

PARAMETERS FOR THE TIME DEPENDENCE AT 675 Å and 825 Å

Run No.	Pressure (Torr)	u_4 (10^6 sec^{-1})	u_5 (10^6 sec^{-1})	A_4	A_5
<u>675 Å</u>					
57	50	0.039	0.011	576	629
27C	100	0.072	0.028	2192	2576
32 ^a	209	0.107	0.020	4456	648
128 ^b	207	0.110	0.042	837	256
176 ^c	202	0.120	0.033	2061	56
185	300	0.219	0.090	2569	614
30	416	0.369	0.031	832	308
35	610	0.617	0.050	2064	368
180	802	1.05	0.119	838	123
231	1006	1.40	0.098	628	20
<u>825 Å</u>					
59	50	0.035	0.009	442	328
28	100	0.081	0.028	1465	1779
33 ^a	209	0.107	0.015	6164	397
133 ^d	208	0.111	0.019	2343	113
177A ^c	202	0.114	0.036	1894	36
188	303	0.198	0.030	3406	94
29	416	0.379	0.030	861	202
36	612	0.596	0.035	2703	112
181	803	1.11	0.076	1224	81
85 ^e	1003	1.42	0.051	2442	96

^a $w = 43.8$ eV per ion pair.^b $w = 42.7$ eV per ion pair.^c $w = 40.0$ eV per ion pair.^d $w = 42.7$ eV per ion pair; 800 Å.^e 800 Å.

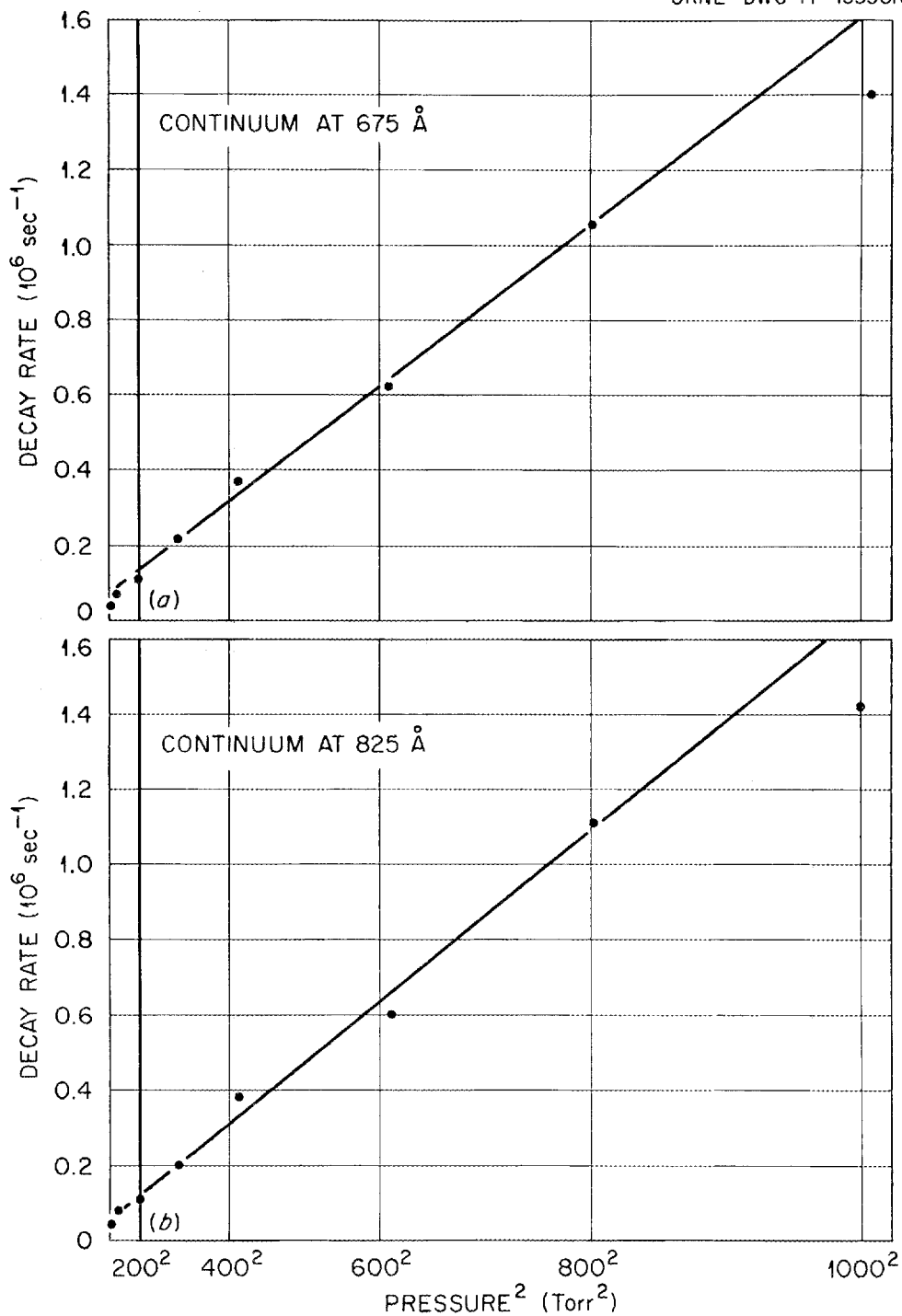


Figure 16. Pressure Dependence of the Decay Rate, u_4 of the Main Component at 675 Å and 825 Å.

TABLE 5

PARAMETERS FOR THE TIME DEPENDENCE OF SOME IMPURITY LINES

Run No.	Wave-length Å	Pressure (Torr)	u_4 (10^6 sec^{-1})	u_5 (10^6 sec^{-1})	A_4	A_5
131	736	209	0.115	0.016	1360	249
132	744	208	0.123	0.008	997	819
136	1025	208	0.099	0	636	403
137	987	208	0.115	0.004	818	206
138	971	210	0.118	0.012	930	299

SECTION 3

THEORY

3.1 The Steps of Radiation Action

Some insight into the first stages of the interaction of protons (1-4 MeV) with helium can be obtained using theoretical techniques. The radiation action may be considered to occur in four steps.^{3,28} In step 1 the proton generates excited atoms, ions, and secondary electrons. In step 2 those secondary (including tertiary, etc.) electrons with sufficient energy induce further excitation and ionization until all the electrons have energies less than the lowest excited atomic state (subexcitation electrons). The third step is the radiative decay of excited atoms to long-lived excited states and to the ground state. In the fourth step the excited atoms, ions, and subexcitation electrons react with each other, with ground state atoms, and with impurities producing excited molecules, Jesse ions, and other species. The first three steps are dealt with in this section, and the fourth is examined later by coupling the theoretical estimates with experimental data.

3.2 Step 1--Primary Ionization and Excitation

Cross sections for the ionization of helium, $\sigma(e, E)$, by protons of energy E yielding an electron of energy e are listed in Tables 6 and 7.

TABLE 6

QUANTUM MECHANICAL DIFFERENTIAL IONIZATION
CROSS SECTIONS FOR PROTONS IN HELIUM

e (eV)	σ (cm ² /eV)		
	1-MeV Proton	2-MeV Proton	4-MeV Proton
0	1.22 (-18)*	7.24 (-19)	4.19 (-19)
2.72	9.77 (-19)	5.79 (-19)	3.35 (-19)
5.44	7.93 (-19)	4.67 (-19)	2.69 (-19)
10.88	5.40 (-19)	3.15 (-19)	1.80 (-19)
16.33	3.83 (-19)	2.21 (-19)	1.25 (-19)
21.77	2.82 (-19)	1.62 (-19)	9.15 (-20)
27.21	2.14 (-19)	1.22 (-19)	6.85 (-20)
32.65	1.67 (-19)	9.43 (-20)	5.25 (-20)
38.09	1.33 (-19)	7.46 (-20)	4.13 (-20)
40.82	1.19 (-19)	6.69 (-20)	3.71 (-20)
47.62	9.32 (-20)	5.18 (-20)	2.85 (-20)
54.42	7.43 (-20)	4.11 (-20)	2.25 (-20)
68.03	4.98 (-20)	2.73 (-20)	1.49 (-20)
81.63	3.53 (-20)	1.91 (-20)	1.03 (-20)
95.24	2.61 (-20)	1.40 (-20)	7.47 (-21)
108.84	2.00 (-20)	1.07 (-20)	5.70 (-21)
136.05	1.31 (-20)	6.93 (-21)	3.66 (-21)
163.26	9.08 (-21)	4.75 (-21)	2.48 (-21)
190.47	6.60 (-21)	3.39 (-21)	1.74 (-21)
217.68	5.02 (-21)	2.60 (-21)	1.35 (-21)
326.52	2.43 (-21)	1.24 (-21)	6.33 (-22)

*Multiply the cross sections by 10 to the power in parenthesis.

TABLE 7
 CLASSICAL DIFFERENTIAL IONIZATION CROSS
 SECTIONS FOR PROTONS IN HELIUM

e (eV)	σ (cm ² /eV)		e (eV)	σ (cm ² /eV)
	1-MeV Proton	4-MeV Proton		4-MeV Proton
217.68	4.96 (-21)*	1.24 (-21)	5000	2.39 (-24)
326.52	2.23 (-21)	5.58 (-22)	5250	2.17 (-24)
435.36	1.26 (-21)	3.15 (-22)	5500	1.98 (-24)
653.04	5.61 (-22)	1.40 (-22)	5750	1.81 (-24)
870.72	3.16 (-22)	7.90 (-23)	6000	1.66 (-24)
1306.08	1.40 (-22)	3.51 (-23)	6250	1.53 (-24)
1500	1.06 (-22)	2.66 (-23)	6500	1.42 (-24)
1750	6.12 (-23)	1.96 (-23)	6750	1.31 (-24)
2000	3.19 (-23)	1.50 (-23)	7000	1.22 (-24)
2250	1.54 (-23)	1.18 (-23)	7250	1.14 (-24)
2500	5.68 (-24)	9.58 (-24)	7500	1.06 (-24)
2750	1.93 (-25)	7.91 (-24)	7750	8.77 (-25)
3000		6.65 (-24)	8000	7.09 (-25)
3250		5.67 (-24)	8250	5.64 (-25)
3500		4.89 (-24)	8500	4.40 (-25)
3750		4.26 (-24)	8750	3.32 (-25)
4000		3.74 (-24)	9000	2.38 (-25)
4250		3.31 (-24)		
4500		2.96 (-24)		
4750		2.65 (-24)		

*Multiply the cross sections by 10 to the power in parenthesis.

The quantum mechanical cross sections are a result of the Born approximation.^{30,31} The cross sections for 4-MeV protons were obtained by using the approximation

$$\sigma(e, E) = \frac{Y(e) \log E + Z(e)}{E}$$

The parameters $Y(e)$ and $Z(e)$ were determined at each secondary electron energy by using the available 1 and 2-MeV cross sections.³⁰ Cross sections for higher secondary electron energies were estimated using the classical binary encounter collision model,³² Table 7.

Cross sections for the excitation of helium by protons are listed in Table 8. Many parameter wave functions were used by Bell³³ et al to find the cross sections for the N^1S ($N = 2$ thru 7), N^1P ($N = 2$ thru 4) and 3^1D excited states. For the remaining cross sections they used a Hartree-Fock representation of the excited states.

3.3 Electrons Slowing Down--Step 2

When a proton loses energy in helium, excited helium atoms, helium ions and secondary electrons are generated. The secondary electrons produced by the protons have an energy range covering thousands of electron volts (Tables 6 and 7). As each secondary electron slows down to subexcitation energy (energy degradation), the energy that it loses goes into ionizing and exciting helium atoms. It is difficult to determine the number of ions and excited states because

TABLE 8

EXCITATION CROSS SECTIONS FOR PROTONS IN HELIUM

STATE	1 MeV (10^{-20} cm ²)	4 MeV (10^{-20} cm ²)
2 ¹ S	39.22	9.935
3 ¹ S	8.833	2.237
4 ¹ S	3.383	.8569
5 ¹ S	1.651	.4182
6 ¹ S	.9279	.2350
7 ¹ S	.6053	.1533
2 ¹ P	502.6	178.8
3 ¹ P	124.2	44.07
4 ¹ P	49.85	17.67
5 ¹ P	24.9	8.57
6 ¹ P	14.2	4.90
3 ¹ D	2.035	.5238
4 ¹ D	1.08	.272
5 ¹ D	.602	.151
6 ¹ D	.363	.0911

the excitation and ionization processes are competing with each other at every step of the energy degradation.

To date there are no published calculations for this specific case of energy degradation. Fano,³⁴ Miller,³⁵ and Alkhazov³⁶ theoretically estimated the number of ions caused by the energy degradation (W value) of electrons in helium. Erskine³⁷ did similar calculations for the energy degradation of fast alpha particles in helium. In order to use the available information for this work, the secondary electrons at each energy were treated individually. Alkhazov's publication was used because (1) he calculated the energy degradation for electrons of many energies and (2) he includes the individual populations of many excited states as well as the number of ions produced.

Alkhazov calculated the energy degradation of electrons using a set of semi-empirical cross sections.³⁸ These cross sections agree with available experimental data for low-energy electrons and convert to theoretical estimates at energies above 500 eV. He did not include processes which involve a change of state of the atoms, such as the formation of molecular (Hornbeck) ions and attachment of electrons to atoms. Examples of his calculated results are reproduced from his publication in Table 9 and Figure 17. The populations that he gives for the 2^1D and 2^3D states were ignored in the present work because these two states cannot occur.

Alkhazov alleged his estimated populations of the

TABLE 9

AVERAGE NUMBER OF ATOMS FORMED IN VARIOUS EXCITED STATES
RESULTING FROM THE ENERGY DEGRADATION OF A 1230-EV ELECTRON

	N = 2	N = 3	N = 4	N > 4
N^1S	1.43	0.29	0.11	0.16
N^1P	7.32	1.73	0.70	1.05
N^1D	0.82	0.19	0.073	0.11
N^3S	2.25	0.22	0.073	0.098
N^3P	1.21	0.20	0.071	0.098
N^3D	0.38	0.063	0.023	0.032

ORNL-DWG 71-13488

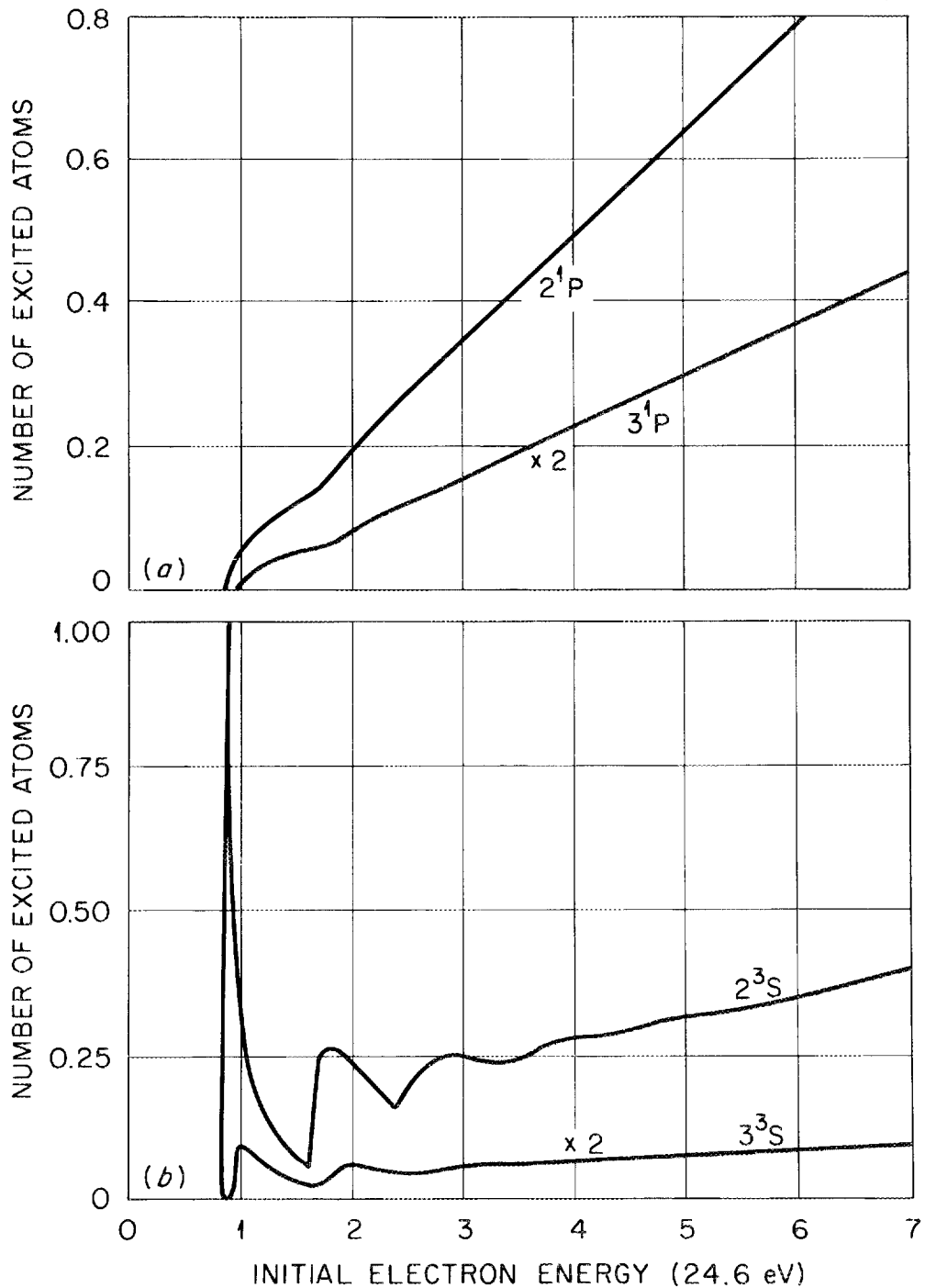


Figure 17. Number of Excited Atoms Per Incident Electron as a Function of Initial Electron Energy.

states corresponding to forbidden transitions might be too high. In fact he provided a second but incomplete set of data using cross sections reduced by a factor of two for states corresponding to forbidden transitions.

The number of helium ions and excited helium atoms resulting from the energy degradation were estimated by combining Alkhazov's data with the theoretical energy distribution of secondary electrons (Tables 6 and 7). An integration was done by the trapezoid technique. Alkhazov's populations were assumed to be linear with electron energy for energies greater than 172 eV.

Figure 18 is a graphic description of steps 1 and 2 of the radiation action of a proton in helium. It was assumed that the proton's energy was constant as it passed through the helium. A more detailed representation is found in Table 10. The products of a 1-MeV proton are scaled (multiplied by the ratio of 4-MeV to 1-MeV stopping powers, 96.6/285), for comparison purposes. The proton induced populations of the N^1S , ($N = 4$ to 6), N^1P , ($N = 4$ to 6), and N^1D , ($N = 4$ to 6) states were estimated using the data of Bell et al³³ (Table 8). The optical approximation²⁸ was used for the N^1P , ($N = 7$ to 12), states. These populations are grouped together and labeled "other atomic levels" in Table 10.

Alkhazov published the populations of the highly excited states ($N > 3$, where N is the principle quantum number) resulting from electron degradation for only one initial

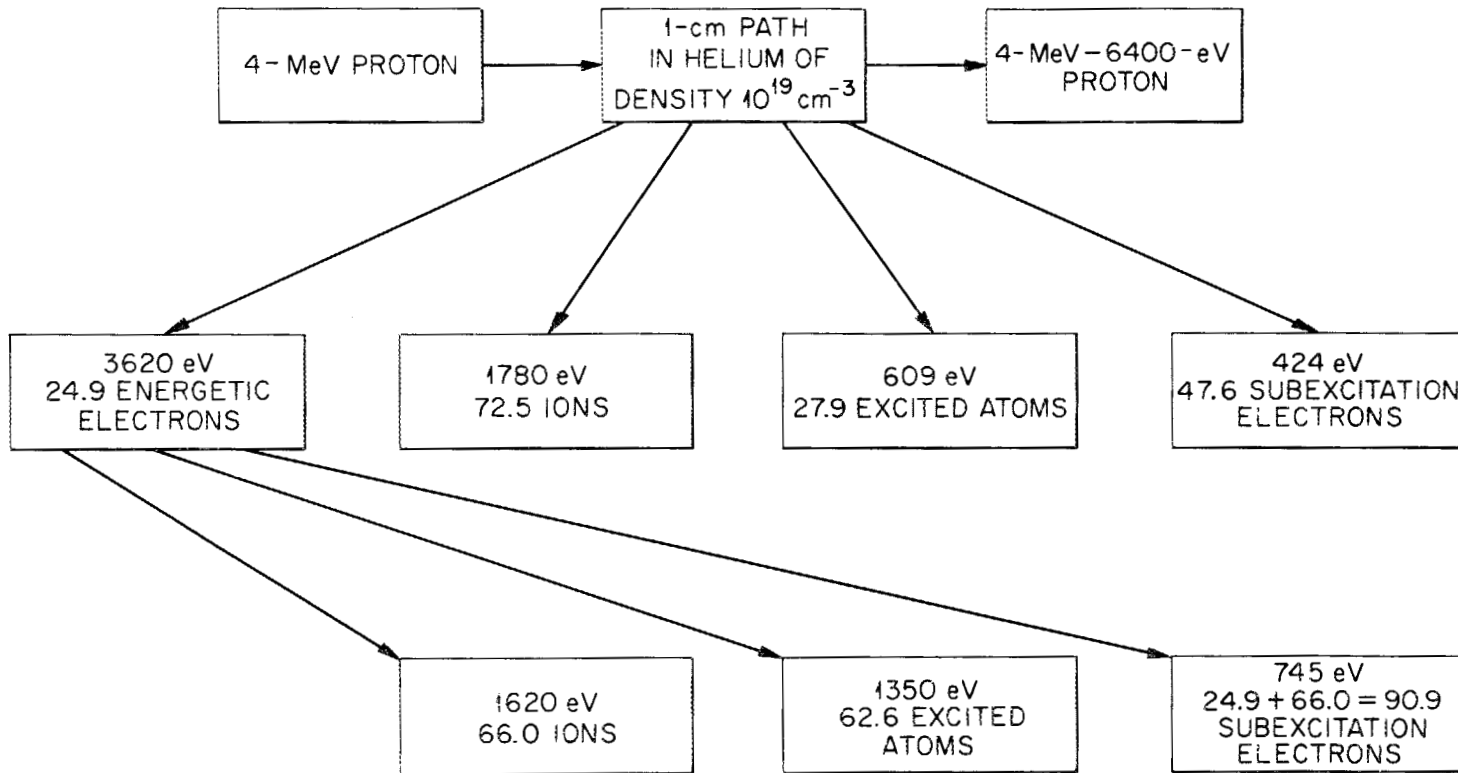


Figure 18. The Energy Degradation When a 4-MeV Proton Loses a Fraction of Its Energy in Helium.

TABLE 10

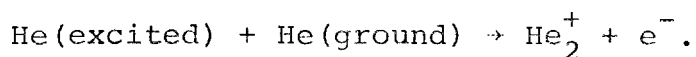
THE AVERAGE POPULATIONS RESULTING WHEN ONE PROTON HAS A
1 cm PATH IN 10^{19} cm^{-3} OF HELIUM

Products	4 MeV Proton		1 MeV Proton (scaled)	
	Primary Proton	Secondary Electrons	Primary Proton	Secondary Electrons
2^1S	0.99	6.24	1.33	6.30
3^1S	0.22	1.21	0.30	1.22
2^1P	17.9	19.5	17.0	18.1
3^1P	4.41	4.47	4.20	4.12
3^1D	0.05	0.73	0.07	0.73
2^3S		11.3		11.5
3^3S		1.10		1.12
2^3P		6.13		6.27
3^3P		1.25		1.31
3^3D		1.31		1.18
Other atomic levels	4.30	9.30	4.25	9.05
Ions	72.5	66.0	76.1	60.2

electron energy (1230 eV), Table 9. The populations of these highly excited states resulting from the degradation of all the secondary electrons were estimated by assuming that the ratio of highly excited state populations ($N > 3$) to lower excited state populations ($N \leq 3$) is constant with respect to initial electron energy.

One way to test the validity of these estimates is to audit them for energy conservation (see Figure 18). The proton ionization and proton excitation cross sections indicate that a 4 MeV proton as it passes through 1 cm of helium with density 10^{19} cm^{-3} will lose $3620 \text{ eV} + 1780 \text{ eV} + 609 \text{ eV} + 424 \text{ eV} = 6430 \text{ eV}$. This agrees with the 6400 eV from Jani's³⁹ tables. The 3620 eV of the energetic electrons are degraded to $1620 \text{ eV} + 1350 \text{ eV} + 745 \text{ eV} = 3720 \text{ eV}$.

The experimentally-determined W value for 4-MeV protons is used to check the accuracy of this work. A W value of $\frac{6430 \text{ eV}}{66.0 + 72.5 \text{ ion pairs}} = 46.4 \text{ eV/ion pairs}$ is calculated. The calculation is not complete since additional ions (Hornbeck⁴⁰ ions) are formed when excited helium atoms collide with ground state atoms. All highly excited states (states with $N > 3$) have sufficient energy to form a Hornbeck ion.⁴¹



It is generally assumed⁴² that the Hornbeck process has competition only from radiative de-excitation, allowing most of the highly excited states to form Hornbeck ions at pressures

above 50 Torr. Contrary to the general assumption, the Hornbeck process may have strong competition from collisional de-excitation, as inferred by Huffman and Katayama⁴³ from their photoionization experiments using argon. The measured W value (45.5 eV/ion pair¹⁷) lies between the W values calculated when the Hornbeck process is neglected (46.4 eV/ion pair) and when the Hornbeck process is taken to be 100% efficient (42.3 eV/ion pair).

Another experiment to be compared with the theory is the $d\epsilon/dx$ measurement of Hurst et al.¹⁸ They determined that 2200 eV of vuv radiation results when a 4-MeV proton passes through 1 cm of helium at 400 Torr. Since the theory is for 283 Torr, the 2200 eV is multiplied by 283/400 (energy lost by the proton is proportional to pressure) and 1560 eV is obtained. The theoretical estimate of atomic excitation energy is 1960 eV. At first this seems too high. However, some of the atomic excitation energy is converted to kinetic energy. This energy conversion occurs when excited helium molecules drop to the ground repulsive molecular state, the measured continuous vuv light is emitted, and the atoms speed away from each other. In addition, the small amount of radiation at optical wavelengths was, of course, not included in the vuv measurements.

In summary, the present work indicates that the energy lost by a 1-MeV and a 4-MeV proton degrades to almost identical end products (Table 10). Also of general interest is

that the secondary electrons play the major role in excitation and ionization. Of particular importance to the energy pathways studies is that 30% of the energy lost by the proton goes into exciting atoms. Of these excited atoms, about half are in the 2^1P state.

3.4 Step 3--Radiative Decay

The radiative decay of the excited states with principle quantum number 2 or 3 is displayed in Figure 21. Decay rates for allowed transitions were obtained from Wiese's⁴⁴ tables. A 20 sec^{-1} decay rate⁴⁵ was used for the 2^1S state. Resonance (involving an allowed transition to the ground state) radiation from the 2^1P and 3^1P states is absorbed and re-emitted (resonance trapped) many times by neighboring ground state atoms before the photon escapes from the gas. The decay rate, β , for these resonance transitions were estimated by using Holstein's⁴⁶ pressure independent decay constant:

$$\beta = \frac{0.2069}{t} (\lambda/R)^{1/2}.$$

Where λ is the wavelength of the emitted light, t is the natural lifetime and R is the radius of the cylindrical gas container. The experimental conditions for this work yield

$$\beta = \frac{5 \times 10^{-4}}{t}.$$

The reader is cautioned not to draw conclusions from

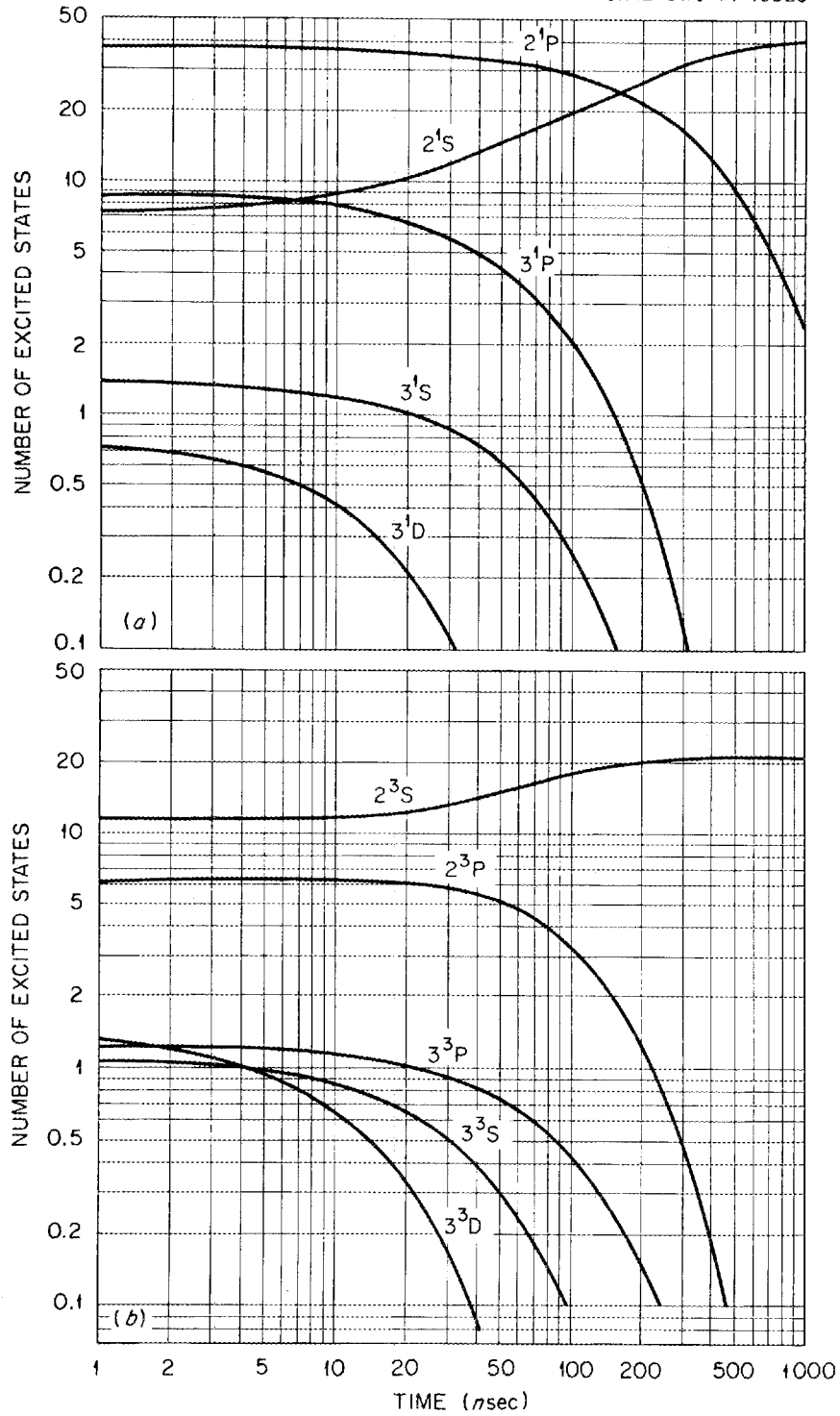


Figure 19. Relative Number of Various Excited States in Helium as a Function of Time.

Figure 19 except at very low pressures. The experimental part of this study shows that the 2^1P states are depleted rapidly by collisions before they can radiate to the 2^1S state.

SECTION 4

POTENTIAL SURFACES

When a proton interacts with helium gas, 30% of the absorbed energy goes into atomic excitation. At normal pressures (100 to 1000 Torr) most of this excitation energy appears as vuv molecular radiation. To better understand the formation and de-excitation of these molecules, the available data on helium's potential surfaces has been combined into one useful diagram (Figure 20).

The task of data compilation for this diagram was lightened by exploiting Ginter and Battino's⁴⁷ recent publication of potential curves which are based mainly on optical spectra. In a private communication Ginter⁴⁸ supplied the vibration frequencies and the coordinates of the minima for the D and $F^1\pi_u$ states. These quantities describe the position and shape of the very bottom of the potential wells. Theoretical estimates by Scott⁴⁹ et al. for the A state show a maximum of 0.153 eV at $2.76 \overset{\circ}{\text{A}}$. The four molecular levels originating from the 2^1P atomic state were calculated by Schweinler⁵⁰ using the dipole-dipole interaction. The three theoretical estimates^{51,52,53} of the ground state are in agreement even though these publications span almost two decades. Jordan and Amdur's⁵⁴ experimental data conform to this same surface. The binding energy of the ground state is small enough (less than 6×10^{-7} eV, 0.005°K)⁵⁵ to be

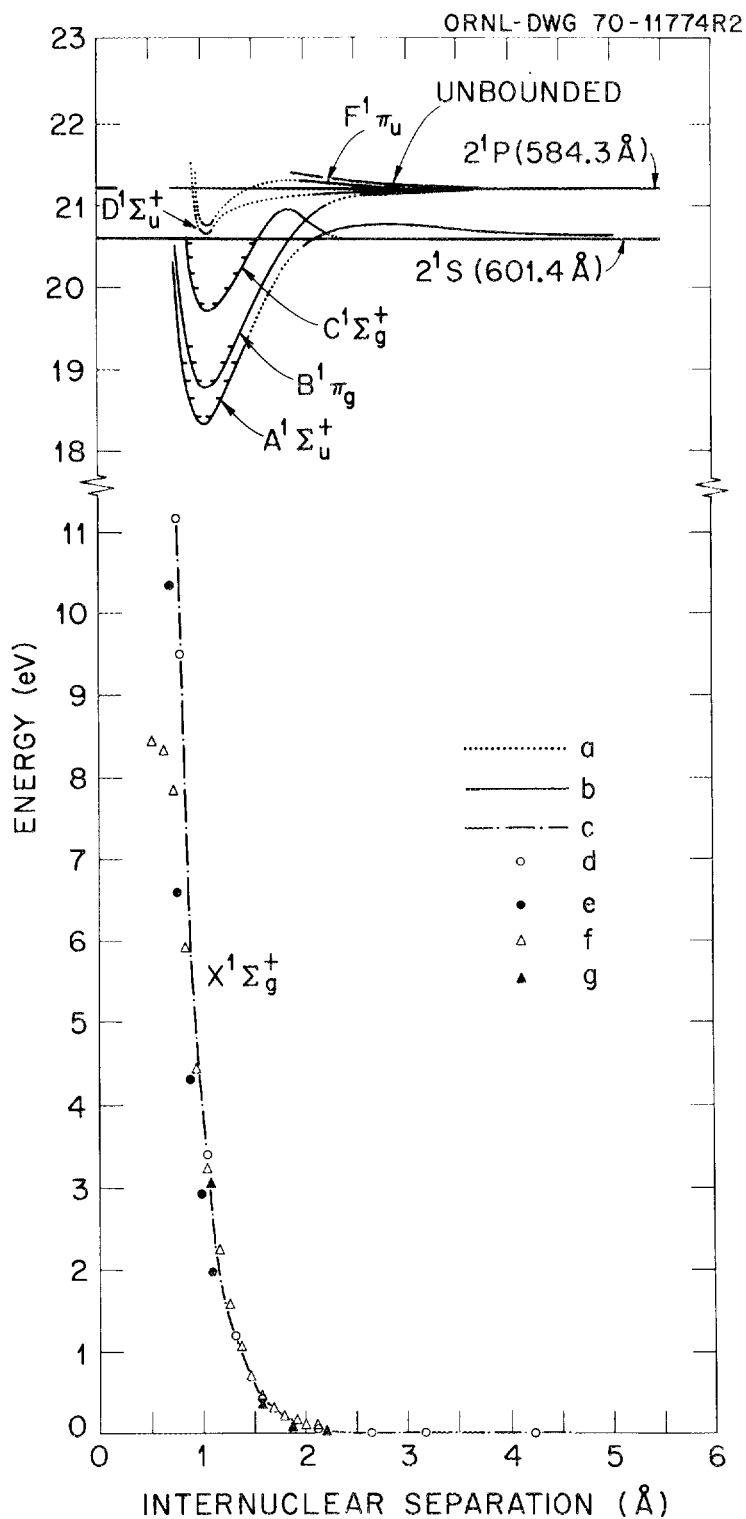


Figure 20. Potential Energy Curves for Selected States of He_2 : (a) Hypothetical curves; (b) refs. 47, 48, 49, and 50; (c) and (d) ref. 51; (e) ref. 54; (f) ref. 53; (g) ref. 52.

neglected in these energy pathways studies.

Several general features can immediately be seen in Figure 22: (1) There are molecular states with substantial binding energy; (2) In order to gain access to the A, F, and C states the colliding atoms must overcome potential barriers; and, (3) Several eV of potential energy is converted to kinetic energy in verticle transitions from excited molecular states to the highly repulsive X state.

SECTION 5

DISCUSSION

5.1 Proposed Model for the Vuv Emission

At the present stage of its development an energy pathways model for helium should be consistent with:

(1) T.E. Stewart's²² vuv emission studies, (2) J.E. Park's¹⁷ Jesse effect measurements, (3) time dependent vuv emission experiments, (4) theoretical treatment of the first stage of radiation action, and (5) potential surface data. In the model suggested (Figure 21) energy from the proton and secondary electrons excite helium atoms to the 2^1P state. At pressures above 50 Torr these excited atoms lose energy by collisions as they form excited metastable molecules. The metastable molecule is de-excited by collision with helium ground state atoms to a radiating molecule which emits the slow component in the vuv continuum.

The first energy pathway in this model is via atomic excitation by protons and secondary electrons. Since about half of these excited atoms are in the 2^1P state (Table 10), the 2^1P state is most likely the main energy source for both the vuv emission and the Jesse effect.

Two well-known energy pathways out of the 2^1P state are via the allowed radiative transitions to the 2^1S ($20,581 \text{ \AA}$) state, and to the ground (584 \AA) state. Other mechanisms depleting the 2^1P state are revealed by observing the pressure

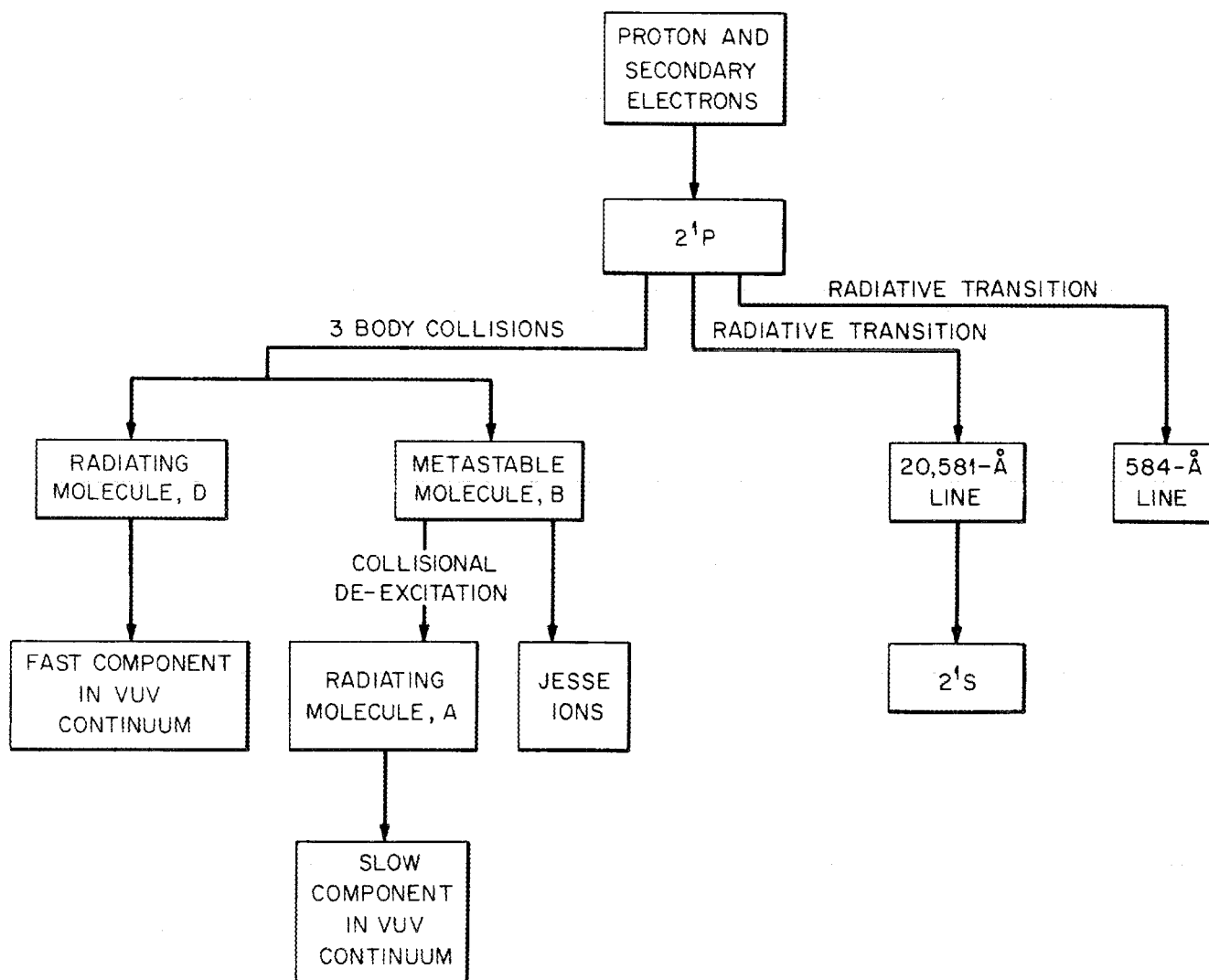
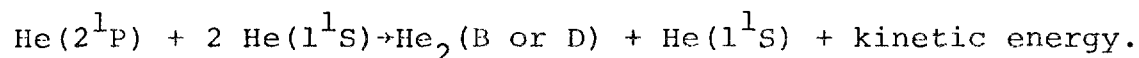


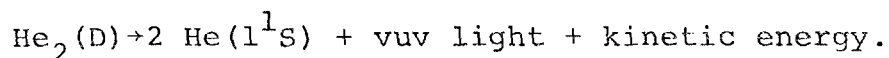
Figure 21. Energy Pathways Model.

dependence of the 2^1P depletion rate as reflected through the $584\text{-}\overset{\circ}{\text{A}}$ line decay rate. This rate varies with pressure (Figure 10). At $584\text{-}\overset{\circ}{\text{A}}$ the intensity divided by pressure decreases with increasing pressure (Figure 22), indicating that collision processes compete with $584\text{-}\overset{\circ}{\text{A}}$ radiation. Intensity divided by pressure is a fundamental parameter since the energy lost by the proton increases linearly with pressure.

The pressure squared (P^2) dependence of the $584\text{-}\overset{\circ}{\text{A}}$ line's decay rate is due to depletion of the 2^1P state by collisions with two ground state helium atoms forming an excited molecule:

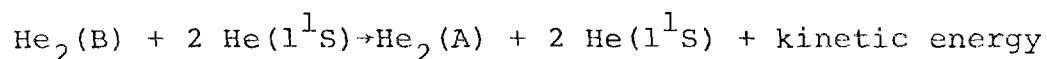


The D and B molecular states (Figure 20) can be readily formed by this process. When the D state radiates to the X state, the fast component in the vuv continuum

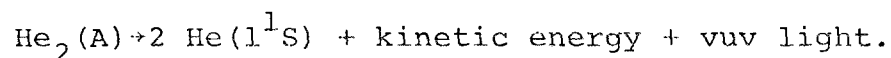


The energy of this radiation (640 to $950 \overset{\circ}{\text{A}}$) is consistent with the D and X potential surfaces (Figure 22).

The rate-determining step for the slow component in the vuv continuum is the collisional de-excitation of the metastable B state to the radiating A state.



The A state then radiates to the X state, i.e.



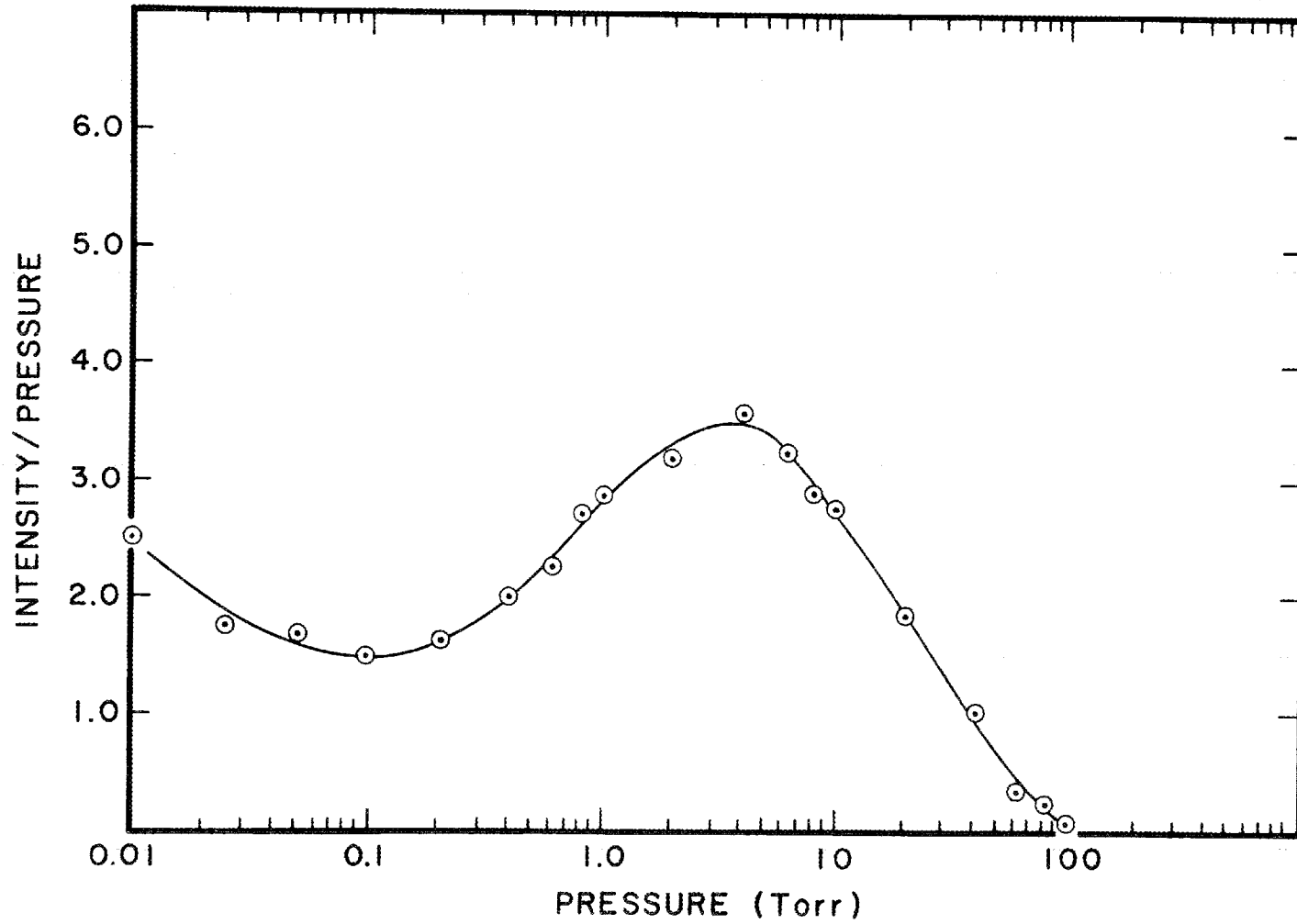


Figure 22. Intensity Divided by Pressure Plotted as a Function of Pressure for the He 584-Å Resonance Line.

Analysis of the A and X potential surfaces (Figure 22) shows that radiation from an A to X transition will have a wavelength between 600 and 1000 Å. The measured lifetime of the slow component is nearly constant with wavelength throughout the continuum indicating a common rate-determining process for the entire region. Between 200 Torr and 800 Torr the decay rate of the continuum is equal to $1.6 P^2$ (Figures 12 and 16) where P is in Torr. This implies that the rate determining step for the slow component is a three-body collision. The rate measured at 1000 Torr deviates from the P^2 straight line. This fact could indicate that the radiation rate of the A state is comparable to the rate of collisional de-excitation when the pressure is 1000 Torr, i.e. comparable to $2 \times 10^6 \text{ sec}^{-1}$.

The above comments on the interpretation of the 584-Å line account only for the P^2 , and not the P term, in the dependence of decay rate on pressure. To attribute the P term to a 2-body radiation process such as Franck-Condon emission is inconsistent with other observations. For example, the 2-body term would be prompt and could be said to be the continuum's fast component. But this is inconsistent with the observation that the ratio of fast component intensity to slow component intensity is constant with pressure. Furthermore, a Franck-Condon continuum originating at the 584-Å line is not seen. We suggest that the linearity in P is only apparent and is merely a combination of a β that is pressure

dependent and the P^2 term.

Atomic states other than 2^1P are excited by the protons and secondary electrons (Table 10). Account should be made for this excitation energy. The 2^1S and 2^3S excited states are depleted slowly by collisions⁵⁶

$$2^1S \text{ depletion rate (sec}^{-1}\text{)} = 200 P(\text{Torr})$$

$$2^3S \text{ depletion rate (sec}^{-1}\text{)} = 0.3 P^2(\text{Torr}^2).$$

This fact could account for the small secondary component in the time dependent spectra of the vuv continuum. The remaining excited states are depleted by processes including molecular formation and radiation cascade to the 2^1P , 2^1S , and 2^3S states. Higher molecular states that radiate to the A, B and D states contribute more intensity to the vuv continuum's fast and slow components.

Samples of Stewart's²² data for the pressure dependence of the vuv emission intensity produced when protons excite helium are shown in Figures 22 and 23. These curves will be commented upon using the present model. The model is consistent with Stewart's $584\text{-}\overset{\circ}{\text{A}}$ data since these data were used as one input to construct the model. As the pressure increases above 200 Torr, the intensity of the vuv continuum at short wavelengths decreases while the intensity at longer wavelengths increases. This intensity variation is due in part to collisional de-excitation to lower vibrational levels within the D, B, and A molecular states, but may be influenced as

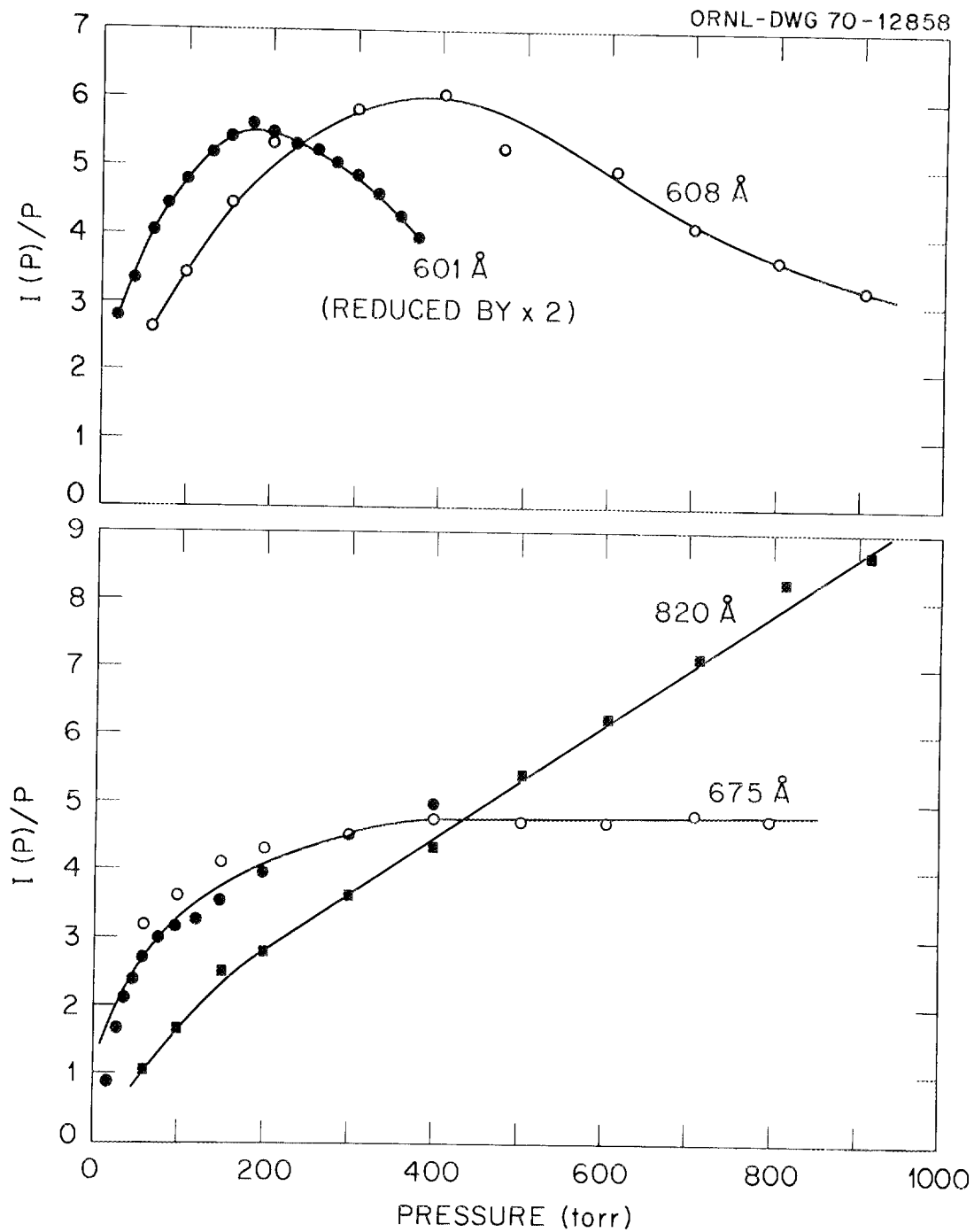


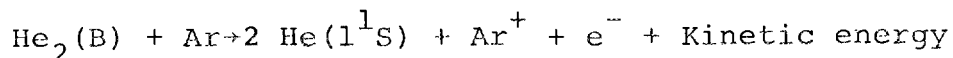
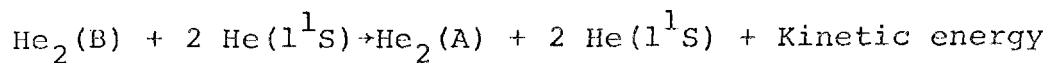
Figure 23. Intensity Divided by Pressure Plotted as a Function of Pressure for the Vuv Emission Continuum of Helium.

well by radiation from higher molecular states.

The necessity of employing a broad experimental program to resolve energy pathways is best illustrated by comparing the present model with an interpretation by Stewart *et al*²² made previous to these time dependent studies. This previous interpretation was based on proton excitation measurements and yet was almost identical to models given by gas discharge investigators.^{7,10,11} It was suggested that the radiation in the 600-Å region is produced from A to X transitions as in the present model. However, it was indicated that the energy pathway to the A state is from the 2^1S atomic state rather than from the B molecular state. The previous interpretation attributed radiation in the 675-Å region to D to X transitions exclusively and the radiation in the 800-Å region to A to X transitions exclusively. Whereas in the present model, radiation throughout the region 601 Å to 950 Å is from A to X transitions with additional radiation in the region 640 Å to 950 Å from D to X transitions.

5.2 Proposed Model for the Jesse Effect

An explanation of the Jesse effect observed when argon is added to helium is derived from the model and from Parks¹⁷ ionization data. A reasonable model would yield a rate which is proportional to the concentration of argon and is of acceptable magnitude. If we assume that the Jesse effect and the collisional de-excitation mechanism are competing processes, we write



The number of ion pairs in the argon-helium mixture, N , is given by

$$N = N_0 + (kP_{\text{Ar}}N^*)/(kP_{\text{Ar}} + \lambda)$$

Where N_0 is the number of ion pairs in the pure gas, k is a proportionality constant to be determined, P_{Ar} is the partial pressure of argon, λ is the de-excitation rate of the metastable molecule ($1.6 P^2$), and N^* is the number of metastable helium molecules, $\text{He}_2(\text{B})$. If we divide by N_0 we obtain

$$N/N_0 = 1 + (kP_{\text{Ar}}N^*/N_0)/(kP_{\text{Ar}} + \lambda)$$

Since $N/N_0 = W_0/W$,

$$W_0/W = 1 + (kP_{\text{Ar}}N^*/N_0)/(kP_{\text{Ar}} + \lambda).$$

Where W_0 is the W value of pure helium (45.5 eV per ion pair¹⁷) and W is the W value of the mixture. When a sufficient amount of argon (about 1% of the volume) is added to helium, the Jesse effect dominates so that W drops to an argon-saturated value W_s . Thus,

$$W_0/W_s = 1 + N^*/N_0.$$

W_s of the mixture is 29.5 eV per ion pair.¹⁷ Thus the quantity N^*/N_0 is obtained and the equation for k is expressed

in terms of experimentally-determined parameters

$$W_o/W = 1 + [kP_{Ar} (W_o/W_s - 1)] / (kP_{Ar} + \lambda).$$

Between 200 and 800 Torr k is about $0.95 \times 10^7 \text{ Torr}^{-1} \text{ sec}^{-1}$ (Table 11) corresponding to a rate constant of $2.7 \times 10^{-10} \text{ cm}^3 \text{ sec}^{-1}$. This rate constant is of the same magnitude as the calculated rate constant⁵⁷ for ionization of argon upon collision with helium atoms in the 2^1P excited state (9.1 to $9.8 \times 10^{-10} \text{ cm}^3 \text{ sec}^{-1}$) and with the measured de-excitation rates⁵⁸ of metastable excited helium atoms (2^1S , $2.2 \times 10^{-10} \text{ cm}^3 \text{ sec}^{-1}$; 2^3S , $0.74 \times 10^{-10} \text{ cm}^3 \text{ sec}^{-1}$).

The magnitude and pressure dependence of the derived Jesse effect rate is encouraging. However, complications, particularly photoionization, are present, as illustrated by comparing the increase in ionization observed ($W = 40 \text{ eV}$) due to natural impurities (Tables 3 and 4) with the increase predicted ($W = 42 \text{ eV}$) using the measured increase in the vuv continuum's decay rate. Before Jesse rates and quenching rates can be directly related, these rates must be measured using known contaminant concentrations in reaction chambers with identical geometries, and under conditions where photoionization contributions can be estimated.

It is possible that the differences in magnitude of Jesse effects in helium with the addition of argon (ionization potential, $IP = 15.8 \text{ eV}$, 787 \AA), krypton ($IP = 14.0 \text{ eV}$, 886 \AA), and xenon ($IP = 12.1 \text{ eV}$, 1022 \AA)⁵⁹ are due to the

TABLE 11

JESSE EFFECT RATE FOR ARGON IN HELIUM

0.00249% Argon in Helium

Total Pressure (Torr)	W(eV/ion pair)	k(10 ⁷ Torr ⁻¹ sec ⁻¹)
59.72	34.43	0.56
80.05	35.89	0.50
108.64	36.19	0.63
204.39	37.64	0.82
305.46	38.77	0.92
411.86	39.53	1.02
502.00	39.92	1.12
602.64	40.72	1.07
705.49	40.84	1.21
812.55	41.61	1.09
910.64	41.91	1.10
1011.68	42.57	0.94

0.0985% Argon in Helium

Total Pressure (Torr)	W(eV/ion pair)	k(10 ⁷ Torr ⁻¹ sec ⁻¹)
104.69	29.72	0.79
202.41	29.96	0.72
302.51	30.09	0.83
410.44	30.33	0.79
506.15	30.37	0.93
607.72	30.56	0.90
704.40	30.69	0.92
812.70	30.77	0.99
902.36	30.86	1.02
1008.90	31.04	1.00

spectrum of energy available from $\text{He}_2(\text{B})$ excited molecules, rather than an effect due to subexcitation electrons.⁶⁰ The spectrum of accessible energy is the difference between the $\text{He}_2(\text{B})$ and $\text{He}_2(\text{X})$ surfaces and is reflected in the vuv emission spectra. Jesse's data for xenon shows about 20 per cent more ion pairs than in argon, and this is compatible with the energy in the vuv spectra.

5.3 General Remarks

One surprising part of this model is the fast depletion rate of the 2^1P state by collisions. Another is that the energy for the Jesse effect in helium is from a molecule rather than an atom.

Experiments that would further establish the validity of this energy pathways model include time dependent studies of the continuum at pressures above 1000 Torr, time dependent quenching studies, time dependent studies of the fast component using apparatus with better time resolution, and time dependent absorption experiments to study the 2^1P depletion rate at pressures from 200 to 1000 Torr.

SECTION 6

SUMMARY

These time dependent studies of the vuv emission from proton-excited helium gas show that the 2^1P state is depleted primarily by collisional process and that the vuv continuum has two components, both of which are pressure dependent. The theoretical estimations illustrate in detail the initial actions when a proton interacts with helium. Molecular helium's potential curves were used extensively in constructing the suggested model. These studies are productive because they can be coupled directly with W value experiments and other emission measurements to yield information on the energy pathways involved in the vuv continuum and in the Jesse effect.

APPENDIX

The raw data for the runs used in the final analysis are listed here. Also listed are a few data repeats (run numbers 24, 25, 39, 53, 89, 122, 135, 153, and 168). The first column is the channel number and the second column is the number of counts in that channel.

PUN NUMBER 24
 MICROSECONDS/CHANNEL 1.03
 WAVELENGTH 675 ANGSTROMS
 PRESSURE 100. TOPP
 PULSE RATE 15.6 KHZ
 W VALUE 41.1 EV/ION PAIR

1	0	16	980	31	520	46	298	61	147
2	0	17	940	32	492	47	263	62	154
3	0	18	920	33	464	48	287	63	136
4	60	19	869	34	465	49	256	64	133
5	114	20	849	35	466	50	226	65	132
6	129	21	781	36	430	51	218	66	129
7	112	22	771	37	430	52	215	67	97
8	121	23	771	38	392	53	210	68	127
9	99	24	743	39	377	54	204	69	103
10	107	25	684	40	344	55	201	70	127
11	92	26	703	41	326	56	190	71	101
12	2033	27	637	42	353	57	162	72	110
13	1213	28	600	43	329	58	191	73	88
14	1112	29	559	44	284	59	168		
15	1135	30	545	45	265	60	163		

PUN NUMBER 25
 MICROSECONDS/CHANNEL 1.03
 WAVELENGTH 601 ANGSTROMS
 PRESSURE 100. TOPP
 PULSE RATE 15.6 KHZ
 W VALUE 41.1 EV/ION PAIR

1	0	16	5210	31	2611	46	1354	61	754
2	0	17	4936	32	2477	47	1334	62	708
3	1	18	4736	33	2293	48	1261	63	703
4	350	19	4490	34	2224	49	1232	64	628
5	556	20	4293	35	2093	50	1197	65	665
6	641	21	4041	36	2143	51	1097	66	587
7	563	22	3887	37	1945	52	1134	67	550
8	544	23	3820	38	1947	53	977	68	535
9	505	24	3697	39	1791	54	985	69	563
10	463	25	3476	40	1834	55	951	70	480
11	448	26	3417	41	1632	56	915	71	489
12	2173	27	3103	42	1648	57	880	72	480
13	5986	28	2916	43	1540	58	838	73	489
14	5834	29	2823	44	1507	59	765		
15	5524	30	2654	45	1460	60	728		

RUN NUMBER 27C
 MICROSECONDS/CHANNEL 1.03
 WAVELENGTH 675 ANGSTROMS
 PRESSURE 100. TORR
 PULSE RATE 15.6 KHZ
 W VALUE 42.3 EV/TON PAIR

1	0	16	4355	31	2163	46	1254	61	777
2	0	17	4088	32	2122	47	1236	62	738
3	0	18	3880	33	2001	48	1151	63	708
4	465	19	3748	34	2018	49	1099	64	702
5	632	20	3549	35	1901	50	1126	65	629
6	700	21	3373	36	1778	51	985	66	644
7	634	22	3329	37	1644	52	1020	67	578
8	605	23	3176	38	1658	53	978	68	568
9	584	24	3074	39	1558	54	949	69	614
10	577	25	2893	40	1484	55	950	70	571
11	544	26	2731	41	1516	56	865	71	533
12	10656	27	2609	42	1472	57	818		
13	4926	28	2581	43	1376	58	790		
14	4791	29	2375	44	1304	59	773		
15	4437	30	2386	45	1244	60	736		

RUN NUMBER 28
 MICROSECONDS/CHANNEL 1.03
 WAVELENGTH 825 ANGSTROMS
 PRESSURE 100. TORR
 PULSE RATE 15.6 KHZ
 W VALUE 42.3 EV/TON PAIR

1	0	16	2990	31	1434	46	832	61	460
2	0	17	2757	32	1377	47	809	62	461
3	0	18	2596	33	1358	48	751	63	466
4	278	19	2445	34	1298	49	715	64	435
5	392	20	2419	35	1198	50	644	65	454
6	451	21	2291	36	1156	51	697	66	403
7	422	22	2141	37	1097	52	664	67	422
8	406	23	2127	38	1066	53	653	68	374
9	398	24	2020	39	1035	54	618	69	382
10	377	25	1900	40	985	55	598	70	366
11	362	26	1792	41	990	56	608	71	385
12	7483	27	1713	42	889	57	532		
13	3376	28	1718	43	952	58	556		
14	3229	29	1546	44	862	59	541		
15	3027	30	1504	45	887	60	499		

RUN NUMBER 29
 NTCFOSECONDS/CHANNEL .258
 WAVELENGTH 825 ANGSTROMS
 PPFSSURE 416. TOFF
 PULSE RATE 62.5 KHZ
 W VALUE 43.8 EV/ION RATE

1	0	16	127	31	542	46	240	61	168	76	132
2	0	17	122	32	489	47	227	62	159	77	131
3	0	18	146	33	478	48	230	63	151	78	125
4	74	19	1234	34	454	49	251	64	175	79	137
5	163	20	2020	35	427	50	222	65	142		
6	183	21	1114	36	404	51	200	66	152		
7	161	22	1016	37	351	52	213	67	157		
8	147	23	984	38	357	53	227	68	140		
9	157	24	850	39	352	54	207	69	147		
10	156	25	874	40	319	55	213	70	133		
11	144	26	812	41	325	56	193	71	154		
12	10152	27	783	42	276	57	180	72	153		
13	125	28	707	43	268	58	150	73	148		
14	1133	29	651	44	279	59	178	74	146		
15	144	30	570	45	244	60	195	75	146		

RUN NUMBER 30
 NTCFOSECONDS/CHANNEL .258
 WAVELENGTH 675 ANGSTROMS
 PPFSSURE 416. TOFF
 PULSE RATE 62.5 KHZ
 W VALUE 43.8 EV/ION RATE

1	0	16	196	31	636	46	334	61	260	76	205
2	0	17	204	32	621	47	333	62	252	77	196
3	0	18	184	33	557	48	341	63	238	78	207
4	144	19	1392	34	530	49	310	64	233	79	207
5	209	20	1896	35	524	50	278	65	229		
6	239	21	1248	36	536	51	302	66	216		
7	265	22	1174	37	489	52	271	67	219		
8	224	23	1066	38	424	53	274	68	219		
9	241	24	996	39	455	54	321	69	213		
10	234	25	967	40	443	55	304	70	215		
11	233	26	896	41	390	56	287	71	195		
12	242	27	784	42	377	57	254	72	233		
13	251	28	741	43	391	58	273	73	230		
14	239	29	676	44	349	59	223	74	205		
15	211	30	623	45	346	60	223	75	201		

PUN NUMBER 31
 MICROSECONDS/CHANNEL .258
 WAVELENGTH 601 ANGSTROMS
 PRESSURE 416. TORR
 PULSE RATE 62.5 KHZ
 W VALUE 43.8 EV/TON PAIR

1	0	16	50	31	863	46	277	61	107	76	57
2	0	17	47	32	807	47	221	62	115	77	60
3	0	18	53	33	741	48	221	63	87	78	74
4	43	19	315	34	602	49	210	64	97	79	52
5	67	20	2246	35	603	50	192	65	113	80	47
6	95	21	2000	36	576	51	188	66	91	81	51
7	66	22	1765	37	537	52	190	67	82	82	48
8	76	23	1728	38	488	53	174	68	77		
9	79	24	1562	39	449	54	160	69	59		
10	63	25	1355	40	392	55	146	70	62		
11	58	26	1367	41	331	56	145	71	66		
12	74	27	1215	42	364	57	113	72	53		
13	54	28	1166	43	342	58	112	73	49		
14	52	29	1030	44	327	59	112	74	155		
15	64	30	852	45	309	60	108	75	57		

PUN NUMBER 32
 MICROSECONDS/CHANNEL 1.03
 WAVELENGTH 675 ANGSTROMS
 PRESSURE 209. TORR
 PULSE RATE 15.6 KHZ
 W VALUE 43.8 EV/TON PAIR

1	0	16	3729	31	1060	46	461	61	279		
2	0	17	3384	32	965	47	413	62	279		
3	0	18	3202	33	922	48	413	63	268		
4	155	19	2935	34	883	49	395	64	232		
5	15360	20	2631	35	750	50	372	65	246		
6	16429	21	2425	36	757	51	377	66	230		
7	10201	22	2244	37	712	52	380				
8	9214	23	2002	38	691	53	360				
9	8102	24	1877	39	599	54	321				
10	6922	25	1649	40	617	55	322				
11	6363	26	1532	41	556	56	303				
12	5738	27	1462	42	556	57	312				
13	5179	28	1360	43	534	58	276				
14	4675	29	1226	44	481	59	268				
15	4031	30	1115	45	460	60	269				

RUN NUMBER 33
 MICROSECONDS/CHANNEL 1.03
 WAVELENGTH 825 ANGSTROMS
 PRESSURE 209. TORR
 PULSE RATE 15.6 KHZ
 W VALUE 43.8 EV/ION PAIR

1	0	16	5389	31	1233	46	412	61	231
2	0	17	4857	32	1180	47	402	62	214
3	1	18	4381	33	1019	48	389	63	218
4	106	19	3902	34	960	49	350	64	181
5	194	20	3576	35	911	50	360	65	198
6	225	21	3254	36	862	51	323	66	199
7	205	22	2857	37	766	52	288	67	174
8	215	23	2609	38	700	53	313	68	217
9	177	24	2369	39	648	54	319	69	188
10	164	25	2108	40	640	55	262	70	193
11	190	26	1933	41	552	56	253	71	176
12	11520	27	1766	42	564	57	266	72	183
13	7326	28	1640	43	522	58	253	73	155
14	6535	29	1497	44	464	59	251		
15	5895	30	1401	45	434	60	237		

RUN NUMBER 34
 MICROSECONDS/CHANNEL 1.03
 WAVELENGTH 601 ANGSTROMS
 PRESSURE 212. TORR
 PULSE RATE 15.6 KHZ
 W VALUE 43.8 EV/ION PAIR

1	0	16	10842	31	2107	46	476	61	180
2	0	17	9322	32	1867	47	479	62	167
3	0	18	8676	33	1761	48	425	63	176
4	75	19	7690	34	1576	49	389	64	145
5	109	20	6664	35	1411	50	372	65	124
6	134	21	6014	36	1242	51	349	66	124
7	160	22	5556	37	1147	52	310	67	137
8	101	23	4893	38	1086	53	296	68	127
9	116	24	4540	39	971	54	276	69	123
10	112	25	3959	40	844	55	251	70	131
11	126	26	3650	41	809	56	221	71	100
12	8748	27	3217	42	706	57	236	72	105
13	15134	28	2908	43	661	58	234	73	101
14	13612	29	2558	44	612	59	168		
15	12041	30	2360	45	552	60	162		

RUN NUMBER 35
 MICROSECONDS/CHANNEL .258
 WAVELENGTH 675 ANGSTROMS
 PRESSURE 610. TORR
 PULSE RATE 62.5 KHZ
 W VALUE 43.4 EV/ION PAIR

1	0	16	181	31	848	46	324	61	226	76	160
2	0	17	165	32	744	47	329	62	213	77	167
3	0	18	10063	33	627	48	295	63	221	78	185
4	0	19	1570	34	610	49	274	64	207	79	178
5	0	20	4681	35	591	50	283	65	203	80	169
6	0	21	2793	36	579	51	246	66	199		
7	0	22	2428	37	458	52	296	67	207		
8	0	23	2119	38	478	53	271	68	225		
9	0	24	1924	39	424	54	246	69	237		
10	0	25	1602	40	435	55	265	70	226		
11	0	26	1525	41	390	56	252	71	205		
12	0	27	1192	42	372	57	209	72	203		
13	194	28	1180	43	370	58	242	73	204		
14	173	29	986	44	313	59	233	74	186		
15	198	30	871	45	310	60	208	75	180		

RUN NUMBER 36
 MICROSECONDS/CHANNEL .258
 WAVELENGTH 825 ANGSTROMS
 PRESSURE 612. TORR
 PULSE RATE 62.5 KHZ
 W VALUE 43.4 EV/ION PAIR

1	0	16	78	31	740	46	164	61	75	76	71
2	0	17	46	32	706	47	162	62	75	77	61
3	0	18	70	33	563	48	137	63	72	78	80
4	34	19	1634	34	518	49	115	64	89	79	81
5	72	20	5967	35	478	50	138	65	84	80	74
6	93	21	3389	36	423	51	111	66	83		
7	74	22	2797	37	360	52	118	67	97		
8	79	23	2511	38	308	53	98	68	81		
9	78	24	2238	39	295	54	97	69	71		
10	69	25	1755	40	273	55	139	70	65		
11	77	26	1590	41	242	56	99	71	72		
12	65	27	1377	42	220	57	103	72	77		
13	73	28	1200	43	193	58	87	73	61		
14	79	29	953	44	181	59	96	74	73		
15	63	30	846	45	179	60	102	75	66		

PUN NUMBER 37
 MICROSECONDS/CHANNEL .258
 WAVELENGTH 601 ANGSTROMS
 PRESSURE 612. TORR
 PULSE RATE 62.5 KHZ
 W VALUE 43.4 EV/ION PAIR

1	0	16	24	31	479	46	81	61	37	76	20
2	0	17	16	32	428	47	58	62	33	77	31
3	0	18	12	33	370	48	65	63	35	78	24
4	12	19	142	34	363	49	63	64	32	79	17
5	19	20	2525	35	312	50	68	65	23	80	26
6	36	21	2371	36	303	51	67	66	37	81	20
7	23	22	2110	37	266	52	41	67	31	82	22
8	33	23	1766	38	199	53	44	68	29		
9	26	24	1468	39	157	54	49	69	26		
10	19	25	1250	40	140	55	43	70	23		
11	18	26	1141	41	111	56	44	71	20		
12	20	27	928	42	92	57	42	72	29		
13	24	28	819	43	106	58	25	73	29		
14	20	29	669	44	105	59	41	74	23		
15	15	30	587	45	78	60	29	75	27		

PUN NUMBER 39
 MICROSECONDS/CHANNEL .0258
 WAVELENGTH 584 ANGSTROMS
 PRESSURE 103. TORR
 PULSE RATE 125. KHZ
 W VALUE 42.2 EV/ION PAIR

1	0	16	194	31	175	46	188	61	236	76	512
2	0	17	177	32	157	47	179	62	974	77	395
3	0	18	183	33	160	48	195	63	2310	78	354
4	115	19	195	34	175	49	171	64	3314	79	376
5	204	20	174	35	195	50	177	65	4098	80	291
6	199	21	151	36	197	51	164	66	3916	81	304
7	200	22	200	37	178	52	192	67	3058	82	275
8	191	23	196	38	179	53	175	68	2438	83	238
9	224	24	173	39	151	54	172	69	1950	84	255
10	177	25	150	40	155	55	147	70	1501	85	243
11	179	26	185	41	167	56	158	71	1256		
12	203	27	187	42	193	57	179	72	982		
13	189	28	204	43	189	58	189	73	784		
14	178	29	172	44	203	59	197	74	684		
15	189	30	166	45	173	60	181	75	616		

RUN NUMBER 45
 MICROSECONDS/CHANNEL .00644
 WAVELENGTH 584 ANGSTROMS
 PRESSURE 50. TORR
 PULSE RATE 125. KHZ
 W VALUE NOT AVAILABLE EV/ION PAIR

1	0	16	1170	31	1241	46	697	61	429	76	231
2	0	17	1254	32	1208	47	684	62	356	77	240
3	0	18	1362	33	1140	48	607	63	403	78	202
4	1	19	1382	34	1102	49	642	64	356	79	228
5	13	20	1524	35	1013	50	595	65	354	80	188
6	9	21	1624	36	1094	51	602	66	336		
7	27	22	1669	37	946	52	619	67	329		
8	97	23	1770	38	1013	53	577	68	288		
9	210	24	1681	39	911	54	567	69	345		
10	357	25	1611	40	902	55	506	70	319		
11	537	26	1521	41	869	56	477	71	259		
12	624	27	1452	42	863	57	474	72	285		
13	801	28	1368	43	848	58	470	73	263		
14	949	29	1354	44	777	59	410	74	244		
15	1028	30	1352	45	761	60	428	75	258		

RUN NUMBER 47
 MICROSECONDS/CHANNEL .0129
 WAVELENGTH 584 ANGSTROMS
 PRESSURE 24.5 TORR
 PULSE RATE 125. KHZ
 W VALUE NOT AVAILABLE EV/ION PAIR

1	0	16	2660	31	1118	46	507	61	209	76	94
2	0	17	2433	32	1065	47	486	62	215	77	85
3	0	18	2345	33	1032	48	421	63	207	78	93
4	10	19	2256	34	940	49	416	64	206	79	89
5	33	20	2156	35	909	50	393	65	179	80	105
6	313	21	2019	36	884	51	387	66	194		
7	820	22	1926	37	845	52	403	67	171		
8	1361	23	1796	38	762	53	349	68	276		
9	1868	24	1751	39	737	54	347	69	145		
10	2228	25	1590	40	650	55	282	70	154		
11	2726	26	1489	41	679	56	284	71	132		
12	2987	27	1431	42	648	57	319	72	146		
13	3169	28	1343	43	605	58	261	73	117		
14	3036	29	1272	44	553	59	257	74	107		
15	2817	30	1205	45	554	60	245	75	122		

PUN NUMBER 53
 MICROSECONDS/CHANNEL 1.03
 WAVELENGTH 675 ANGSTROMS
 PRESSURE 51. TORR
 PULSE RATE 7.81 KHZ
 W VALUE 42.2 EV/ION PAIR

1	0	16	604	31	454	46	320	61	254	76	239
2	0	17	522	32	456	47	326	62	256	77	205
3	0	18	547	33	414	48	310	63	267	78	190
4	66	19	589	34	364	49	307	64	238	79	182
5	96	20	555	35	386	50	329	65	261	80	207
6	1305	21	539	36	425	51	345	66	241	81	188
7	783	22	529	37	393	52	297	67	240	82	209
8	694	23	507	38	346	53	311	68	217		
9	694	24	484	39	375	54	283	69	219		
10	694	25	490	40	432	55	278	70	220		
11	650	26	507	41	324	56	302	71	260		
12	621	27	494	42	388	57	286	72	236		
13	601	28	446	43	374	58	268	73	200		
14	571	29	489	44	341	59	272	74	255		
15	619	30	434	45	341	60	266	75	202		

PUN NUMBER 55A
 MICROSECONDS/CHANNEL 1.03
 WAVELENGTH 601 ANGSTROMS
 PRESSURE 51. TORR
 PULSE RATE 7.81 KHZ
 W VALUE 42.2 EV/ION PAIR

1	0	16	1398	31	1000	46	774	61	610	76	464
2	0	17	1363	32	1008	47	769	62	609	77	465
3	0	18	1361	33	946	48	744	63	573	78	502
4	88	19	1315	34	981	49	713	64	577	79	511
5	201	20	1320	35	966	50	705	65	579	80	438
6	623	21	1319	36	947	51	675	66	589	81	491
7	1763	22	1293	37	938	52	718	67	555	82	459
8	1751	23	1225	38	905	53	697	68	535		
9	1684	24	1255	39	919	54	743	69	571		
10	1564	25	1114	40	907	55	726	70	555		
11	1609	26	1106	41	793	56	752	71	527		
12	1655	27	1101	42	858	57	618	72	544		
13	1522	28	1114	43	779	58	635	73	509		
14	1470	29	1139	44	885	59	662	74	500		
15	1351	30	1086	45	783	60	655	75	471		

RUN NUMBER 55B
 MICROSECONDS/CHANNEL .00644
 WAVELENGTH 584 ANGSTROMS
 PRESSURE 151. TOPP
 PULSE RATE 125. KHZ
 W VALUE NOT AVAILABLE EV/TON PAIR

1	0	16	1063	31	919	46	270	61	133	76	66
2	0	17	1197	32	820	47	260	62	125	77	67
3	1357	18	1334	33	706	48	232	63	112		
4	5	19	1339	34	714	49	259	64	111		
5	0	20	1468	35	622	50	241	65	95		
6	175	21	1503	36	545	51	175	66	107		
7	36	22	1567	37	525	52	173	67	97		
8	48	23	1593	38	470	53	172	68	106		
9	107	24	1608	39	482	54	122	69	82		
10	211	25	1479	40	398	55	163	70	93		
11	383	26	1336	41	392	56	145	71	66		
12	549	27	1241	42	366	57	137	72	74		
13	730	28	1204	43	335	58	140	73	81		
14	867	29	1015	44	324	59	119	74	74		
15	939	30	971	45	297	60	116	75	76		

RUN NUMBER 56
 MICROSECONDS/CHANNEL .0258
 WAVELENGTH 584 ANGSTROMS
 PRESSURE 10. TOPP
 PULSE RATE 125. KHZ
 W VALUE NOT AVAILABLE EV/TON PAIR

1	0	16	1556	31	397	46	117	61	37		
2	0	17	1460	32	345	47	104	62	30		
3	2	18	1366	33	332	48	90	63	23		
4	1	19	1203	34	305	49	74	64	27		
5	4	20	1051	35	277	50	70	65	25		
6	272	21	968	36	267	51	61	66	20		
7	1105	22	895	37	256	52	67	67	19		
8	2015	23	789	38	203	53	62	68	20		
9	2706	24	794	39	191	54	49	69	17		
10	2804	25	660	40	189	55	59	70	15		
11	2550	26	608	41	169	56	52	71	23		
12	2341	27	574	42	135	57	52	72	11		
13	2088	28	560	43	154	58	48	73	14		
14	1932	29	472	44	117	59	53	74	12		
15	1690	30	418	45	114	60	34	75	10		

RUN NUMBER 57
 MICROSFCONDS/CHANNEL 1.03
 WAVELENGTH 675 ANGSTROMS
 PRESSURE 50. TORR
 PULSE RATE 7.81 KHZ
 W VALUE 40.9 EV/TON PAIR

1	0	16	1132	31	716	46	528	61	436	76	322
2	0	17	983	32	713	47	567	62	415		
3	2	18	912	33	715	48	531	63	403		
4	67	19	942	34	664	49	484	64	412		
5	179	20	898	35	635	50	501	65	392		
6	632	21	962	36	642	51	504	66	406		
7	2551	22	907	37	685	52	454	67	364		
8	1267	23	863	38	665	53	473	68	393		
9	1239	24	879	39	669	54	495	69	350		
10	1188	25	795	40	595	55	463	70	367		
11	1142	26	852	41	588	56	468	71	352		
12	1099	27	788	42	597	57	419	72	358		
13	1033	28	742	43	573	58	452	73	346		
14	1090	29	744	44	531	59	495	74	348		
15	1002	30	742	45	571	60	438	75	344		

RUN NUMBER 59
 MICROSFCONDS/CHANNEL 1.03
 WAVELENGTH 825 ANGSTROMS
 PRESSURE 50. TORR
 PULSE RATE 7.81 KHZ
 W VALUE 40.9 EV/TON PAIR

1	0	16	642	31	472	46	324	61	279	76	214
2	0	17	612	32	520	47	356	62	245		
3	18	18	642	33	459	48	315	63	243		
4	13	19	621	34	431	49	298	64	265		
5	126	20	572	35	433	50	341	65	279		
6	107	21	575	36	410	51	327	66	260		
7	2144	22	513	37	429	52	307	67	261		
8	760	23	546	38	444	53	335	68	208		
9	757	24	551	39	381	54	334	69	256		
10	779	25	558	40	387	55	310	70	236		
11	754	26	517	41	441	56	328	71	258		
12	711	27	486	42	367	57	257	72	253		
13	704	28	502	43	377	58	299	73	219		
14	672	29	476	44	346	59	260	74	210		
15	691	30	460	45	345	60	285	75	215		

RUN NUMBER 74
 MICROSECONDS/CHANNEL .129
 WAVELENGTH 601 ANGSTROMS
 PRESSURE 1002. TOFF
 PULSE RATE 125. 5HZ
 W VALUE 43.3 EV/ION PAIF

1	0	16	1043	31	79	46	35
2	0	17	857	32	69	47	17
3	0	18	659	33	82	48	24
4	12	19	602	34	58	49	30
5	17	20	509	35	69	50	23
6	22	21	453	36	51		
7	22	22	380	37	68		
8	25	23	273	38	41		
9	15	24	256	39	48		
10	28	25	246	40	43		
11	1306	26	158	41	34		
12	2277	27	154	42	39		
13	1833	28	118	43	36		
14	1548	29	112	44	14		
15	1200	30	89	45	31		

RUN NUMBER 85
 MICROSECONDS/CHANNEL .103
 WAVELENGTH 800 ANGSTROMS
 PRESSURE 1003. TOFF
 PULSE RATE 125. KHZ
 W VALUE 43.0 EV/ION PAIF

1	0	16	1974	31	287	46	89	61	81
2	0	17	1694	32	249	47	86	62	77
3	0	18	1450	33	249	48	106	63	78
4	31	19	1225	34	227	49	81	64	91
5	59	20	1125	35	226	50	80	65	84
6	62	21	970	36	193	51	96	66	69
7	66	22	859	37	155	52	88	67	70
8	75	23	732	38	158	53	87	68	67
9	55	24	595	39	131	54	86	69	69
10	53	25	581	40	158	55	96	70	69
11	65	26	505	41	142	56	68		
12	4030	27	443	42	139	57	99		
13	3588	28	402	43	125	58	81		
14	2553	29	390	44	117	59	90		
15	2218	30	297	45	109	60	83		

RUN NUMBER 89
 MICRSECONDS/CHANNEL .0644
 WAVELENGTH 800 ANGSTROMS
 PRESSURE 1008. TOPP
 PULSE RATE 125. KHZ
 W VALUE 43.0 EV/TON DATA

1	0	16	414	31	588	46	196	61	78	76	55
2	0	17	410	32	536	47	200	62	91	77	71
3	0	18	630	33	512	48	193	63	97	78	75
4	892	19	2328	34	449	49	135	64	83	79	56
5	882	20	1963	35	382	50	159	65	80	80	68
6	974	21	1336	36	389	51	125	66	80		
7	888	22	1218	37	361	52	157	67	60		
8	801	23	1072	38	325	53	132	68	72		
9	721	24	1018	39	293	54	113	69	83		
10	620	25	940	40	299	55	127	70	73		
11	576	26	851	41	277	56	107	71	82		
12	493	27	811	42	251	57	116	72	76		
13	473	28	700	43	243	58	103	73	72		
14	595	29	672	44	233	59	99	74	62		
15	528	30	633	45	244	60	78	75	58		

RUN NUMBER 122
 MICRSECONDS/CHANNEL 1.03
 WAVELENGTH 601 ANGSTROMS
 PRESSURE 204. TOPP
 PULSE RATE 15.6 KHZ
 W VALUE 42.7 EV/TON DATA

1	0	16	1713	31	317	46	83	61	28		
2	0	17	1507	32	280	47	77	62	25		
3	0	18	1380	33	243	48	66	63	21		
4	7	19	1195	34	245	49	58	64	18		
5	15	20	1089	35	202	50	50	65	28		
6	24	21	930	36	189	51	41	66	22		
7	22	22	833	37	189	52	55	67	18		
8	14	23	769	38	157	53	43	68	21		
9	21	24	674	39	139	54	41	69	16		
10	38	25	594	40	134	55	40	70	20		
11	2885	26	520	41	103	56	36	71	15		
12	2842	27	498	42	107	57	29				
13	2425	28	506	43	99	58	28				
14	2142	29	393	44	108	59	29				
15	1947	30	340	45	86	60	31				

RUN NUMBER 123
 MICROSECONDS/CHANNEL 1.03
 WAVELENGTH 601 ANGSTROMS
 PRESSURE 206. TORR
 PULSE RATE 15.6 KHZ
 W VALUE 42.7 EV/ION PAIR

1	0	16	8394	31	1640	46	346	61	116
2	0	17	7195	32	1402	47	353	62	88
3	0	18	6679	33	1244	48	296	63	108
4	58	19	5832	34	1145	49	276	64	102
5	91	20	5169	35	1121	50	255	65	109
6	100	21	4674	36	1013	51	235	66	80
7	88	22	4122	37	832	52	236	67	109
8	89	23	3706	38	768	53	228	68	88
9	75	24	3357	39	709	54	192	69	92
10	141	25	3024	40	644	55	190	70	83
11	13833	26	2571	41	558	56	197	71	67
12	14018	27	2396	42	503	57	167		
13	11987	28	2093	43	488	58	133		
14	10782	29	1924	44	421	59	127		
15	9152	30	1715	45	380	60	122		

RUN NUMBER 124
 MICROSECONDS/CHANNEL 1.03
 WAVELENGTH 596 ANGSTROMS
 PRESSURE 201. TORR
 PULSE RATE 15.6 KHZ
 W VALUE 42.7 EV/ION PAIR

1	0	16	4983	31	951	46	225	61	65
2	0	17	4376	32	861	47	179	62	52
3	0	18	4115	33	762	48	181	63	60
4	25	19	3559	34	695	49	185	64	62
5	64	20	3157	35	639	50	126	65	53
6	75	21	2875	36	579	51	140	66	52
7	49	22	2516	37	504	52	130	67	47
8	55	23	2276	38	511	53	126	68	53
9	42	24	2111	39	384	54	125	69	49
10	84	25	1845	40	395	55	84	70	44
11	8154	26	1581	41	340	56	94	71	51
12	8202	27	1479	42	347	57	89		
13	7208	28	1344	43	299	58	103		
14	6400	29	1187	44	273	59	81		
15	5660	30	1035	45	228	60	71		

RUN NUMBER 125
 MICROSECONDS/CHANNEL 1.03
 WAVELENGTH 605 ANGSTROMS
 PRESSURE 208. TORR
 PULSE RATE 15.6 KHZ
 W VALUE 42.7 EV/ION PAIR

1	0	16	4435	31	786	46	189	61	66
2	0	17	3844	32	740	47	187	62	49
3	0	18	3479	33	697	48	157	63	60
4	30	19	3031	34	589	49	140	64	66
5	35	20	2723	35	556	50	122	65	45
6	52	21	2521	36	512	51	133	66	57
7	48	22	2115	37	450	52	101	67	38
8	44	23	1985	38	396	53	96	68	42
9	48	24	1734	39	382	54	95	69	41
10	63	25	1645	40	329	55	105	70	53
11	7281	26	1472	41	292	56	95	71	36
12	7185	27	1258	42	258	57	86		
13	6207	28	1084	43	216	58	84		
14	5540	29	1032	44	228	59	82		
15	4849	30	935	45	183	60	70		

RUN NUMBER 126
 MICROSECONDS/CHANNEL 1.03
 WAVELENGTH 620 ANGSTROMS
 PRESSURE 208. TORR
 PULSE RATE 15.6 KHZ
 W VALUE 42.7 EV/ION PAIR

1	0	16	1441	31	290	46	74	61	28
2	0	17	1258	32	228	47	63	62	25
3	0	18	1124	33	195	48	59	63	26
4	17	19	971	34	219	49	59	64	27
5	26	20	864	35	153	50	61	65	29
6	26	21	800	36	169	51	64	66	21
7	18	22	721	37	141	52	49	67	25
8	23	23	628	38	151	53	47	68	24
9	23	24	614	39	122	54	46	69	26
10	84	25	512	40	122	55	45	70	14
11	2743	26	446	41	99	56	37	71	15
12	2344	27	459	42	99	57	25		
13	1895	28	389	43	92	58	38		
14	1686	29	328	44	98	59	39		
15	1671	30	299	45	71	60	22		

RUN NUMBER 128
 MICROSECONDS/CHANNEL 1.03
 WAVELENGTH 675 ANGSTROMS
 PRESSURE 207. TORR
 PULSE RATE 15.6 KHZ
 W VALUE 42.7 EV/ION PAIR

1	0	16	802	31	206	46	82	61	15
2	0	17	724	32	206	47	81	62	43
3	0	18	667	33	192	48	70	63	77
4	17	19	617	34	181	49	64	64	34
5	35	20	573	35	144	50	67	65	52
6	34	21	496	36	162	51	66	66	41
7	33	22	483	37	144	52	74	67	31
8	32	23	432	38	119	53	65	68	29
9	37	24	394	39	114	54	53	69	32
10	192	25	359	40	105	55	62	70	44
11	2536	26	332	41	102	56	39		
12	1283	27	271	42	104	57	59		
13	1135	28	283	43	92	58	51		
14	1063	29	261	44	107	59	47		
15	969	30	235	45	75	60	48		

RUN NUMBER 133
 MICROSECONDS/CHANNEL 1.03
 WAVELENGTH 800 ANGSTROMS
 PRESSURE 208. TORR
 PULSE RATE 15.6 KHZ
 W VALUE 42.7 EV/ION PAIR

1	0	16	1804	31	367	46	117	61	56
2	0	17	1600	32	325	47	111	62	35
3	0	18	1369	33	313	48	91	63	51
4	24	19	1305	34	318	49	93	64	57
5	41	20	1119	35	231	50	99	65	39
6	45	21	1049	36	224	51	93	66	44
7	58	22	930	37	214	52	92	67	48
8	48	23	854	38	191	53	69	68	40
9	39	24	730	39	208	54	68	69	51
10	431	25	696	40	176	55	72	70	49
11	5513	26	629	41	182	56	72	71	46
12	2938	27	571	42	160	57	68		
13	2542	28	455	43	143	58	58		
14	2196	29	427	44	138	59	65		
15	2026	30	435	45	126	60	63		

PUN NUMBER 135
 MICROSECONDS/CHANNEL 1.03
 WAVELENGTH 850 ANGSTROMS
 PRESSURE 206. TORR
 PULSE RATE 15.6 KHZ
 W VALUE 42.7 EV/ION PAIR

1	0	16	1564	31	299	46	95	61	56
2	0	17	1400	32	274	47	97	62	37
3	0	18	1253	33	289	48	78	63	54
4	21	19	1034	34	249	49	96	64	47
5	28	20	981	35	210	50	71	65	46
6	42	21	886	36	204	51	67	66	32
7	35	22	785	37	206	52	51	67	47
8	39	23	728	38	185	53	61	68	49
9	26	24	656	39	151	54	70	69	33
10	110	25	588	40	128	55	54	70	26
11	4585	26	541	41	141	56	65	71	36
12	2391	27	437	42	140	57	42		
13	2166	28	379	43	120	58	60		
14	1912	29	357	44	103	59	57		
15	1685	30	336	45	132	60	50		

PUN NUMBER 140
 MICROSECONDS/CHANNEL 1.03
 WAVELENGTH 601 ANGSTROMS
 PRESSURE 102. TORR
 PULSE RATE 7.81 KHZ
 W VALUE 42.7 EV/ION PAIR

1	0	16	4495	31	2294	46	1241	61	756	76	434
2	0	17	4122	32	2114	47	1162	62	709	77	410
3	0	18	4005	33	2051	48	1169	63	654	78	390
4	36	19	3814	34	1983	49	1096	64	648	79	385
5	93	20	3639	35	1899	50	1053	65	592	80	353
6	83	21	3432	36	1853	51	997	66	549	81	351
7	88	22	3383	37	1694	52	941	67	568		
8	81	23	3174	38	1723	53	940	68	565		
9	10090	24	3079	39	1585	54	937	69	484		
10	77	25	2920	40	1507	55	888	70	481		
11	4488	26	2778	41	1525	56	854	71	502		
12	5350	27	2650	42	1458	57	832	72	461		
13	5073	28	2668	43	1465	58	797	73	501		
14	4852	29	2577	44	1321	59	757	74	426		
15	4583	30	2316	45	1337	60	721	75	443		

RUN NUMBER 153
 MICROSECONDS/CHANNEL .0129
 WAVELENGTH 584 ANGSTROMS
 PRESSURE 71.2 TORR
 PULSE RATE 125. KHZ
 W VALUE NOT AVAILABLE EV/ION PAIR

1	0	16	238	31	923	46	265	61	69
2	0	17	552	32	887	47	220	62	55
3	0	18	920	33	785	48	195	63	60
4	10	19	1195	34	758	49	190	64	66
5	12	20	1463	35	701	50	160	65	57
6	9	21	1787	36	594	51	133	66	63
7	9	22	1913	37	565	52	171	67	40
8	11	23	2070	38	492	53	135	68	45
9	14	24	1970	39	465	54	104	69	39
10	14	25	1786	40	404	55	116	70	30
11	106	26	1634	41	393	56	109	71	35
12	6	27	1460	42	394	57	91	72	35
13	17	28	1321	43	348	58	102	73	28
14	13	29	1174	44	311	59	76	74	27
15	25	30	1113	45	272	60	82	75	22

RUN NUMBER 154
 MICROSECONDS/CHANNEL .0129
 WAVELENGTH 584 ANGSTROMS
 PRESSURE 102. TORR
 PULSE RATE 125. KHZ
 W VALUE NOT AVAILABLE EV/ION PAIR

1	0	16	347	31	816	46	138	61	40	76	22
2	0	17	745	32	717	47	132	62	44	77	26
3	0	18	1070	33	642	48	120	63	34	78	29
4	26	19	1458	34	569	49	108	64	38	79	31
5	16	20	1731	35	487	50	124	65	29		
6	15	21	1996	36	443	51	74	66	36		
7	17	22	2141	37	375	52	96	67	30		
8	9	23	2176	38	347	53	68	68	35		
9	17	24	1964	39	320	54	63	69	25		
10	15	25	1837	40	288	55	77	70	34		
11	18	26	1612	41	275	56	56	71	23		
12	20	27	1404	42	216	57	47	72	33		
13	8	28	1168	43	197	58	55	73	27		
14	15	29	1055	44	181	59	47	74	23		
15	10060	30	887	45	173	60	43	75	27		

RUN NUMBER 155
 MICROSECONDS/CHANNEL .0129
 WAVELENGTH 584 ANGSTROMS
 PRESSURE 121. TORR
 PULSE RATE 125. KHZ
 W VALUE NOT AVAILABLE EV/ION PAIR

1	0	16	352	31	583	46	98	61	39	76	24
2	0	17	719	32	479	47	79	62	36	77	25
3	0	18	964	33	440	48	58	63	38	78	30
4	12	19	1274	34	358	49	65	64	34	79	21
5	20	20	1440	35	312	50	61	65	27	80	28
6	17	21	1684	36	289	51	61	66	24		
7	20	22	1835	37	230	52	51	67	27		
8	16	23	1835	38	232	53	49	68	37		
9	19	24	1622	39	190	54	60	69	38		
10	17	25	1394	40	156	55	32	70	22		
11	17	26	1143	41	156	56	38	71	30		
12	13	27	956	42	140	57	32	72	30		
13	21	28	888	43	125	58	28	73	31		
14	22	29	766	44	119	59	41	74	35		
15	88	30	639	45	112	60	32	75	29		

RUN NUMBER 156
 MICROSECONDS/CHANNEL .0129
 WAVELENGTH 584 ANGSTROMS
 PRESSURE 135. TORR
 PULSE RATE 125. KHZ
 W VALUE NOT AVAILABLE EV/ION PAIR

1	0	16	366	31	432	46	62	61	31	76	31
2	0	17	644	32	371	47	57	62	37	77	41
3	0	18	956	33	329	48	48	63	31	78	26
4	18	19	1182	34	316	49	45	64	35	79	23
5	14	20	1342	35	257	50	43	65	21	80	34
6	18	21	1510	36	196	51	39	66	41		
7	21	22	1565	37	187	52	45	67	32		
8	13	23	1593	38	164	53	43	68	38		
9	20	24	1382	39	153	54	34	69	24		
10	19	25	1195	40	103	55	43	70	26		
11	22	26	1025	41	110	56	34	71	28		
12	19	27	836	42	96	57	35	72	33		
13	18	28	758	43	86	58	32	73	22		
14	19	29	620	44	97	59	29	74	37		
15	82	30	512	45	67	60	37	75	24		

RUN NUMBER 157
 MICROSECONDS/CHANNEL .0129
 WAVELENGTH 584 ANGSTROMS
 PRESSURE 5.4 TOFF
 PULSE RATE 125. KHZ
 W VALUE NOT AVAILABLE EV/ION PAIR

1	0	16	150	31	746	46	423	61	238	76	118
2	0	17	267	32	812	47	420	62	244	77	121
3	0	18	408	33	710	48	383	63	224	78	117
4	0	19	572	34	651	49	388	64	210	79	113
5	1	20	766	35	647	50	371	65	223	80	98
6	1	21	881	36	625	51	335	66	186		
7	1	22	1028	37	631	52	332	67	180		
8	3	23	1080	38	614	53	316	68	182		
9	1	24	1072	39	515	54	350	69	172		
10	0	25	977	40	529	55	319	70	164		
11	0	26	1018	41	501	56	256	71	167		
12	0	27	968	42	513	57	269	72	130		
13	0	28	969	43	462	58	264	73	151		
14	2	29	887	44	470	59	266	74	130		
15	30	30	812	45	439	60	272	75	135		

RUN NUMBER 158
 MICROSECONDS/CHANNEL .0129
 WAVELENGTH 584 ANGSTROMS
 PRESSURE 86.3 TOFF
 PULSE RATE 125. KHZ
 W VALUE NOT AVAILABLE EV/ION PAIR

1	0	16	457	31	1050	46	228	61	35	76	31
2	0	17	884	32	952	47	203	62	66	77	22
3	0	18	1318	33	846	48	189	63	40	78	25
4	16	19	1690	34	794	49	162	64	49	79	29
5	13	20	1966	35	659	50	155	65	29	80	23
6	13	21	2390	36	635	51	121	66	33		
7	19	22	2441	37	565	52	112	67	38		
8	19	23	2565	38	490	53	109	68	37		
9	25	24	2362	39	430	54	94	69	44		
10	9	25	2029	40	373	55	83	70	27		
11	14	26	1923	41	355	56	73	71	32		
12	18	27	1636	42	290	57	71	72	36		
13	14	28	1488	43	278	58	51	73	23		
14	25	29	1321	44	241	59	54	74	37		
15	100	30	1151	45	256	60	58	75	27		

RUN NUMBER 168
 MICROSECONDS/CHANNEL .0258
 WAVELENGTH 584 ANGSTROMS
 PRESSURE 10. TOPP
 PULSE RATE 125. KHZ
 W VALUE NOT AVAILABLE EV/ION PAIR

1	0	16	1480	31	377	46	111	61	26	76	13
2	0	17	1284	32	335	47	85	62	34	77	9
3	0	18	1313	33	321	48	80	63	21	78	10
4	0	19	1130	34	295	49	81	64	16	79	7
5	2	20	977	35	291	50	68	65	17	80	4
6	2	21	904	36	251	51	80	66	20	81	14
7	1	22	869	37	236	52	68	67	14	82	9
8	1	23	783	38	222	53	61	68	12		
9	0	24	737	39	182	54	53	69	15		
10	2	25	668	40	159	55	46	70	13		
11	0	26	643	41	166	56	48	71	15		
12	44	27	586	42	145	57	38	72	10		
13	370	28	522	43	123	58	34	73	11		
14	709	29	452	44	121	59	22	74	13		
15	1204	30	417	45	110	60	32	75	7		

RUN NUMBER 175
 MICROSECONDS/CHANNEL 1.03
 WAVELENGTH 601 ANGSTROMS
 PRESSURE 202. TOPP
 PULSE RATE 15.6 KHZ
 W VALUE 40.0 EV/ION PAIR

1	0	16	4706	31	812	46	159	61	46		
2	0	17	4182	32	702	47	127	62	52		
3	0	18	3762	33	625	48	130	63	50		
4	16	19	3241	34	574	49	103	64	35		
5	28	20	2887	35	509	50	96	65	28		
6	28	21	2605	36	418	51	81	66	43		
7	26	22	2283	37	400	52	86	67	23		
8	24	23	2054	38	379	53	82	68	26		
9	18	24	1750	39	316	54	80	69	26		
10	163	25	1586	40	285	55	66	70	24		
11	8481	26	1450	41	252	56	61	71	17		
12	7813	27	1278	42	232	57	51				
13	6807	28	1159	43	232	58	45				
14	6264	29	1000	44	176	59	44				
15	5473	30	873	45	151	60	42				

RUN NUMBER 176
 MICROSECONDS/CHANNEL 1.03
 WAVELENGTH 675 ANGSTROMS
 PRESSURE 202. TORR
 PULSE RATE 15.6 KHZ
 W VALUE 40.0 EV/ION PAIR

1	0	16	1369	31	268	46	42	61	19
2	0	17	1237	32	221	47	56	62	18
3	0	18	1232	33	208	48	31	63	18
4	6	19	967	34	206	49	37	64	17
5	13	20	889	35	174	50	42	65	13
6	8	21	758	36	135	51	36	66	12
7	7	22	694	37	146	52	41	67	11
8	5	23	647	38	109	53	31	68	13
9	11	24	590	39	95	54	33	69	8
10	103	25	471	40	90	55	20	70	8
11	4694	26	457	41	81	56	27	71	13
12	2306	27	364	42	96	57	17		
13	2003	28	317	43	79	58	16		
14	1769	29	325	44	78	59	18		
15	2595	30	282	45	77	60	19		

RUN NUMBER 177A
 MICROSECONDS/CHANNEL 1.03
 WAVELENGTH 825 ANGSTROMS
 PRESSURE 202. TORR
 PULSE RATE 15.6 KHZ
 W VALUE 40.0 EV/ION PAIR

1	0	16	1393	31	245	46	53	61	16
2	0	17	1194	32	220	47	49	62	17
3	0	18	1098	33	200	48	46	63	16
4	4	19	933	34	174	49	33	64	9
5	12	20	830	35	141	50	32	65	11
6	14	21	771	36	147	51	31	66	9
7	10	22	694	37	130	52	27	67	15
8	13	23	606	38	106	53	21	68	12
9	8	24	513	39	108	54	25	69	7
10	33	25	479	40	90	55	21	70	5
11	4408	26	450	41	90	56	13	71	6
12	2170	27	382	42	71	57	18		
13	1961	28	314	43	73	58	13		
14	1683	29	296	44	62	59	17		
15	1609	30	279	45	46	60	15		

RUN NUMBER 179
 MICROSECONDS/CHANNEL .0644
 WAVELENGTH 601 ANGSTROMS
 PRESSURE 803. TORR
 PULSE RATE 125. KHZ
 W VALUE 41.8 EV/ION PAIR

1	0	16	842	31	302	46	129	61	63	76	39
2	0	17	754	32	291	47	117	62	54	77	34
3	0	18	712	33	244	48	105	63	55	78	35
4	358	19	666	34	240	49	122	64	46	79	28
5	414	20	582	35	216	50	106	65	45	80	29
6	442	21	565	36	216	51	81	66	37	81	36
7	501	22	547	37	212	52	95	67	43	82	36
8	1172	23	476	38	181	53	96	68	35	83	30
9	1441	24	470	39	164	54	87	69	39		
10	1278	25	409	40	191	55	89	70	36		
11	1205	26	415	41	148	56	70	71	32		
12	1098	27	371	42	127	57	64	72	37		
13	1044	28	317	43	134	58	69	73	29		
14	933	29	355	44	138	59	63	74	40		
15	883	30	310	45	114	60	59	75	31		

RUN NUMBER 180
 MICROSECONDS/CHANNEL .0644
 WAVELENGTH 675 ANGSTROMS
 PRESSURE 802. TORR
 PULSE RATE 125. KHZ
 W VALUE 42.4 EV/ION PAIR

1	0	16	643	31	281	46	198	61	103	76	93
2	0	17	651	32	276	47	146	62	109	77	98
3	100	18	583	33	265	48	176	63	107	78	78
4	282	19	559	34	254	49	115	64	113	79	86
5	349	20	531	35	299	50	156	65	108	80	80
6	405	21	467	36	243	51	139	66	74		
7	829	22	521	37	243	52	151	67	84		
8	2182	23	424	38	212	53	168	68	97		
9	1143	24	436	39	238	54	139	69	80		
10	993	25	410	40	225	55	149	70	113		
11	1024	26	382	41	214	56	118	71	101		
12	853	27	353	42	199	57	131	72	100		
13	803	28	349	43	211	58	112	73	71		
14	763	29	317	44	176	59	110	74	82		
15	735	30	333	45	176	60	106	75	94		

PUN NUMBER 181
 MICROSECONDS/CHANNEL .0644
 WAVELENGTH 825 ANGSTROMS
 PRESSURE 803. TORR
 PULSE RATE 125. KHZ
 W VALUE 42.4 EV/ION PAIR

1	0	16	889	31	382	46	156	61	78	76	71
2	0	17	861	32	363	47	173	62	106	77	76
3	0	18	839	33	316	48	178	63	110	78	69
4	441	19	722	34	320	49	145	64	93	79	174
5	482	20	684	35	297	50	129	65	183	80	61
6	478	21	646	36	301	51	131	66	86		
7	985	22	626	37	254	52	150	67	63		
8	3275	23	573	38	246	53	133	68	83		
9	1966	24	593	39	241	54	119	69	80		
10	1450	25	542	40	219	55	118	70	80		
11	1382	26	485	41	181	56	130	71	68		
12	1288	27	501	42	195	57	101	72	80		
13	1141	28	403	43	182	58	99	73	65		
14	1109	29	397	44	212	59	116	74	72		
15	1007	30	403	45	138	60	99	75	60		

PUN NUMBER 185
 MICROSECONDS/CHANNEL 1.03
 WAVELENGTH 675 ANGSTROMS
 PRESSURE 300. TORR
 PULSE RATE 31.3 KHZ
 W VALUE 41.9 EV/ION PAIR

1	0	16	1720	31	212	46	2127	61	180		
2	0	17	1369	32	118	47	1757	62	173		
3	0	18	1159	33	109	48	1508	63	150		
4	51	19	983	34	108	49	1189	64	135		
5	68	20	802	35	75	50	1071	65	113		
6	82	21	666	36	82	51	870	66	100		
7	90	22	575	37	61	52	756	67	92		
8	61	23	469	38	72	53	580	68	80		
9	71	24	415	39	55	54	518	69	57		
10	64	25	375	40	72	55	410	70	63		
11	7214	26	276	41	68	56	380	71	61		
12	3842	27	282	42	6400	57	327				
13	3210	28	193	43	3784	58	248				
14	2550	29	104	44	3173	59	235				
15	2071	30	171	45	2599	60	189				

RUN NUMBER 186
 MICROSECONDS/CHANNEL 1.03
 WAVELENGTH 601 ANGSTROMS
 PRESSURE 301. TOFF
 PULSE RATE 31.3 KHZ
 W VALUE 41.9 EV/ION PAIR

1	0	16	0	31	0	46	7411	61	390
2	0	17	0	32	0	47	5892	62	357
3	0	18	0	33	0	48	4996	63	300
4	0	19	0	34	0	49	3909	64	265
5	0	20	0	35	0	50	3365	65	199
6	0	21	0	36	0	51	2730	66	170
7	0	22	0	37	141	52	2283	67	134
8	0	23	0	38	116	53	1815	68	137
9	0	24	0	39	81	54	1502	69	118
10	0	25	0	40	90	55	1235	70	93
11	0	26	0	41	205	56	1053	71	83
12	0	27	0	42	12228	57	836		
13	0	28	0	43	13610	58	719		
14	0	29	0	44	11293	59	556		
15	0	30	0	45	9037	60	446		

RUN NUMBER 188
 MICROSECONDS/CHANNEL 1.03
 WAVELENGTH 825 ANGSTROMS
 PRESSURE 303. TOFF
 PULSE RATE 31.3 KHZ
 W VALUE 41.9 EV/ION PAIR

1	0	16	1817	31	179	46	2325	61	155
2	0	17	1424	32	115	47	1824	62	145
3	0	18	1180	33	87	48	1585	63	130
4	37	19	945	34	77	49	1326	64	112
5	77	20	764	35	77	50	1037	65	107
6	77	21	702	36	77	51	892	66	75
7	67	22	484	37	55	52	787	67	91
8	44	23	476	38	75	53	619	68	70
9	56	24	406	39	59	54	505	69	53
10	49	25	330	40	42	55	437	70	63
11	7325	26	264	41	79	56	362	71	57
12	4339	27	230	42	6591	57	305		
13	3360	28	209	43	4245	58	234		
14	2814	29	106	44	3582	59	220		
15	2212	30	135	45	2896	60	164		

RUN NUMBER 231
 MICROSECONDS/CHANNEL .117
 WAVELENGTH 675 ANGSTROMS
 PRESSURE 1006. TOPP
 PULSE RATE 125. KHZ
 W VALUE 42.5 EV/TON PAIR

1	0	16	413	31	50	46	28	61	26
2	0	17	327	32	42	47	21	62	10
3	4	18	288	33	39	48	15	63	8
4	13	19	239	34	29	49	16	64	8
5	18	20	241	35	41	50	14	65	17
6	13	21	173	36	34	51	23	66	16
7	16	22	154	37	28	52	10	67	12
8	8	23	149	38	29	53	14	68	7
9	10	24	114	39	26	54	19	69	12
10	8	25	82	40	26	55	17	70	10
11	1442	26	95	41	21	56	11	71	15
12	851	27	59	42	20	57	14	72	8
13	666	28	62	43	24	58	16	73	10
14	583	29	68	44	19	59	12		
15	505	30	47	45	10	60	19		

REFERENCES

1. T.E. Bortner and G.S. Hurst, Phys. Rev. 93, 1236 (1954).
2. W.P. Jesse, and J. Sadauskis, Phys. Rev. 88, 417 (1952).
3. G.S. Hurst, T.E. Bortner, and R.E. Glick, J. Chem. Phys. 42, 713 (1965).
4. J.J. Hopfield, Astrophys 72, 133 (1930).
5. J.L. Nickerson, Phys. Rev. 47, 707 (1935).
6. Y. Tanaka, JOSA 45, 710 (1955).
7. Y. Tanaka, A.S. Jursa, and F.J. LeBlanc, JOSA 48, 304 (1958).
8. R.E. Huffman, Y. Tanaka, and J.C. Larrabee, JOSA 52, 851 (1962).
9. R.E. Huffman, Y. Tanaka, and J.C. Larrabee, Appl. Opt. 2, 617 (1963).
10. Y. Tanaka, and K. Yoshino, J. Chem. Phys. 39, 3081 (1963).
11. D. Villarejo, R.R. Herm, and M.G. Inghram, JOSA 56, 1574 (1966).
12. S. Kubota, T. Takahashi, and T. Doke, Phys. Rev. 165, 225 (1968).
13. C.Z. van Doorn and J.H. Haanstra, Appl. Opt. 7, 1655 (1968).
14. R.C. Michaelson, and A.L. Smith, Chemical Physics Letters 6, 1 (1970).
15. K.M. Sando, Proc. VI Conf. on the Physics of Electronic and Atomic Collisions, Cambridge, Mass. (M.I.T. Press, 1969) p. 894.
16. F.H. Mies, and A.L. Smith, J. Chem. Phys. 45, 994 (1966).
17. J.E. Parks, Dissertation, University of Kentucky, 1970.
18. T.E. Stewart, G.S. Hurst, T.E. Bortner, J.E. Parks, F.W. Martin, and H.L. Weidner, JOSA 60, 1290 (1970).
19. T.E. Stewart, Dissertation, University of Kentucky, 1970.

20. G.S. Hurst, T.E. Bortner, and T.D. Strickler, J. Chem. Phys. 49, 2460 (1968).
21. G.S. Hurst, T.E. Bortner, and T.D. Strickler, Phys. Rev. 178, 4 (1969).
22. T.E. Stewart, G.S. Hurst, D.M. Bartell, and J.E. Parks, Phys. Rev. A 3, 1991 (1971).
23. G.S. Hurst, T.E. Stewart, and J.E. Parks, Phys. Rev. A 2, 1717 (1970).
24. T.E. Stewart, J.E. Parks, G.S. Hurst, T.E. Bortner, and F.W. Martin, in abstracts of The 22nd Gaseous Electronics Conference and High Pressure Arc Symposium, Gatlinburg, Tennessee (Oak Ridge National Laboratory, 1969) p. 80.
25. N. Thonnard and G.S. Hurst, Phys. Rev. A 5, 1110 (1972).
26. H.L. Weidner, unpublished.
27. The amplifier and discriminator were designed and constructed by H. Holzer, Physics Department, University of Kentucky, Lexington, Kentucky.
28. R.L. Platzman, The Vortex 23, 1 (1962).
29. P.J. Walsh, Phys. Rev. 116, 511 (1959).
30. A.E. Kingston, private communication.
31. K.L. Bell, and A.E. Kingston, J. Phys. B 2, 653 (1969).
32. L. Vriens, Proc. Phys. Soc. 90, 935 (1967).
33. K.L. Bell, D.J. Kennedy, and A.E. Kingston, J. Phys. B 1, 1037 (1968).
34. U. Fano, Phys. Rev. 70, 44 (1946).
35. W.F. Miller, Dissertation, Purdue University, 1956.
36. G.D. Alkazov, "Calculating the Slowing-Down Process of Non-relativistic Electrons in Helium", Ioffe Institute of Physics and Technology, Leningrad, Report FTI-108 (1968), translated from the Russian by Scientific Translation Service, sTs Order No. 7926.
37. G.A. Erskine, Proc. Roy. Soc. A224, 362 (1954).

38. G.D. Alkhozov, *Sov. Phys.-Tech. Phys.* 15, 66 (1970).
39. J.F. Janni, "Calculations of Energy, Range, Pathlength, Straggling, Multiple Scattering and the Probability of Inelastic Nuclear Collisions for 0.1 to 1000 MeV Protons," Air Force Weapons Laboratory Technical Report No. AFWL-TR-65-150 (1966).
40. J.A. Hornbeck and J.P. Molnar, *Phys. Rev.* 84, 621 (1951).
41. R.K. Curran, *J. Chem. Phys.* 38, 2974 (1963).
42. J.S. Dahler, J.L. Franklin, M.S.B. Munson, and F.H. Field, *J. Chem. Phys.* 36, 3332 (1962).
43. R.E. Huffman, and D.H. Katayama, *J. Chem. Phys.* 45, 138 (1966).
44. W.L. Wiese, M.W. Smith, and B.M. Glennon, Atomic Transition Probabilities, NBS NSRDS 4 Vol. 1 (U.S. Dept. of Comm., Washington, D.C., 1966).
45. R.S. Van Dyck, Jr., C.E. Johnson, and H.A. Shugart, *Phys. Rev. A* 4, 1327 (1971).
46. T. Holstein, *Phys. Rev.* 83, 1159 (1951).
47. M.L. Ginter, and R. Battino, *J. Chem. Phys.* 52, 4469 (1970).
48. M.L. Ginter, private communication.
49. C.R. Scott, E.M. Greenawalt, J.C. Browne, and F.A. Matsen, *J. Chem. Phys.* 47, 4862 (1967).
50. H.C. Schweinler, unpublished data.
51. D.J. Klein, C.E. Rodriguez, J.C. Browne, and F.A. Matsen, *J. Chem. Phys.* 47, 4862 (1967).
52. N. Moore, *J. Chem. Phys.* 33, 471 (1960).
53. P. Rosen, *J. Chem. Phys.* 18, 1182 (1950).
54. J.E. Jordan, and I. Amdur, *J. Chem. Phys.* 46, 165 (1967).
55. D.E. Beck, *J. Chem. Phys.* 50, 541 (1969).
56. A.V. Phelps, *Phys. Rev.* 99, 1307 (1955).
57. T. Watanabe and K. Katsuura, *J. Chem. Phys.* 47, 800 (1967)

58. A.L. Schmeltekopf, and F.C. Fehsenfeld, J. Chem. Phys. 53, 3173 (1970).
59. W.P. Jesse, and J. Sadauskis, Phys. Rev. 100, 1755 (1955).
60. R.L. Platzman, Rad. Res. 2, 1 (1955).

INTERNAL DISTRIBUTION

- | | |
|--------------------------------------|-----------------------|
| 1. Biology Library | 46-95. G. S. Hurst |
| 2-4. Central Research Library | 96. G. D. Kerr |
| 5. Document Reference Section | 97. C. E. Klots |
| 6. Reactor Division Library | 98. J. L. Liverman |
| 7-31. Laboratory Records Dept. (LRD) | 99. K. Z. Morgan |
| 32. Laboratory Records (ORNL-RC) | 100. D. R. Nelson |
| 33. ORNL Patent Office | 101. M. G. Payne |
| 34-35. Y-12 Technical Library | 102. R. H. Ritchie |
| 36. J. A. Auxier | 103. H. C. Schweinler |
| 37. C. F. Barnett | 104. W. S. Snyder |
| 38. R. D. Birkhoff | 105. J. A. Stockdale |
| 39. T. A. Carlson | 106. J. H. Thorngate |
| 40. L. G. Christophorou | 107-116. E. B. Wagner |
| 41. R. N. Compton | 117. C. D. Cooper (C) |
| 42. S. Datz | 118. G. Cowper (C) |
| 43. F. J. Davis | 119. E. Gerjuoy (C) |
| 44. W. R. Garrett | 120. J. L. Magee (C) |
| 45. F. F. Haywood | |

EXTERNAL DISTRIBUTION

121. Peter Ausloos, Radiation Chemistry Branch, National Bureau of Standards, Gaithersburg, Maryland 20760.
122. Miss Margaret Bailey, Division of Biology and Medicine, U. S. Atomic Energy Commission, Washington, D. C. 20545.
- 123-127. D. M. Bartell, Dept. of Physics, University of Western Ontario London 72, Ontario, Canada.
128. J. W. Boring, Research Lab of Engineering Science, University of Virginia, Charlottesville, Va. 22901.
129. T. E. Bortner, 100 Endicott Lane, Oak Ridge, Tennessee 37830.
130. Werner Brandt, Dept. of Physics, New York University, New York, N. Y. 10003.
131. R. S. Caswell, Radiation Physics Laboratory, National Bureau of Standards, Washington, D. C. 20234.
132. Joseph C. Y. Chen, Inst. for Radiation Physics and Aerodynamics University of California, LaJolla, California 92037.
133. P. J. Chantry, Westinghouse Research Laboratories, Pittsburgh, Pa. 15235
134. L. W. Cochran, Administration Bldg., University of Kentucky, Lexington, Ky. 40506.

135. R. W. Crompton, Research School of Physical Sciences, The Australian National University, Ion Diffusion Unit, Box 4, P. O. , Canberra, A. C. T. 2600 Australia.
136. Dwight C. Conway, Dept. of Chemistry, Texas A and M University, College Station, Texas 77843.
137. W. A. Glass, Battelle Northwest Labs, P. O. Box 999, Richland, Washington 99352.
138. R. E. Glick, Inst. of Molecular Biophysics, Florida State University, Tallahassee, Florida 32306.
139. B. R. Gossick, Dept. of Physics, University of Kentucky, Lexington, Ky. 40506.
140. Alex E. S. Green, Dept. of Physics and Astronomy, University of Florida, Gainesville, Florida 32601.
141. G. Herzberg, National Research Council, 100 Sussex Dr. , Ottawa 2, Ontario, Canada.
142. R. H. Huebner, Argonne National Laboratory, 9700 S. Cass Avenue, Argonne, Illinois 60439.
143. Mitio Inokuti, Radiation Physics Division, Argonne National Laboratory, 9700 S. Cass Avenue, Argonne, Illinois 60439.
144. H. C. Jacobson, Dept. of Physics, University of Tennessee, Knoxville, Tennessee 37916.
145. William P. Jesse, St. Procopius College, Physical Sciences Laboratory, Lisle, Illinois 60532.
146. R. Katz, Dept. of Physics, University of Nebraska, Lincoln, Nebraska, 68508.
147. R. E. Knight, Dept. of Physics, University of Kentucky, Lexington, Kentucky 40506.
148. H. A. Koehler, Lawrence Radiation Laboratory, P. O. Box 808, Livermore, California 94550.
149. E. N. Lassettre, Mellon Institute, 4400 Fifth Avenue, Pittsburgh, Pa. 15213.
150. P. K. Leichner, Dept. of Physics, University of Kentucky, Lexington, Kentucky 40506.
151. S. Lipsky, Dept. of Chemistry, University of Minnesota, Minneapolis, Minnesota 55455.
152. D. C. Lorents, Stanford Research Institute, Menlo Park, California 94025.
153. E. W. McDaniel, Georgia Inst. of Technology, School of Physics, Atlanta, Ga. 30332
154. J. W. McGowan, Dept. of Physics, University of Western Ontario, London 72, Ontario, Canada.
155. G. G. Meisels, Dept. of Chemistry, University of Houston, Houston, Texas 77004.
156. C. E. Melton, Dept. of Chemistry, University of Georgia, Athens, Ga. 30601.

157. E. E. Muschlitz, Jr., Dept. of Chemistry, University of Florida, Gainesville, Florida 32601.
158. J. E. Parks, Dept. of Physics, Western Kentucky University, Bowling Green, Kentucky 42101.
159. J. C. Person, Bldg. 203, Argonne National Laboratory, 9700 S. Cass Avenue, Argonne, Illinois 60439.
160. A. V. Phelps, Joint Institute for Laboratory Astrophysics, University of Colorado, Boulder, Colorado 80302.
161. H. H. Rossi, Radiological Research Laboratory, Columbia University, 630 West 168th St., New York, N. Y. 10032.
162. G. J. Schulz, Mason Laboratory, Yale University, 400 Temple St., New Haven, Connecticut 06520.
163. T. E. Stewart, Dept. of Physics and Mathematics, Tennessee A and I State University, Nashville, Tennessee 37203.
164. N. Thonnard, Dept. of Terrestrial Magnetism, Carnegie Institute of Washington, 5241 Broad Branch Rd., NW, Washington, D.C. 20015.
165. D. A. Vroom, Gulf Radiation Technology, Gulf General Atomic, Inc., P. O. Box 608, San Diego, California 92112.
166. ORAU Library.
- 167-168. ORAU Fellowship Office.
169. Laboratory and University Division, ORO.
- 170-171. Technical Information Center (TIC).